

Contents lists available at ScienceDirect

Journal of Constructional Steel Research

journal homepage: www.elsevier.com/locate/jcsr



Comparative assessment of retrofit strategies for progressive collapse mitigation in steel-framed structures

Luca Possidente^a, Fabio Freddi^{a,*}, Ahmed Y. Elghazouli^{b,c}

- ^a Department of Civil, Environmental & Geomatic Engineering, University College London, London, UK
- ^b Department of Civil & Environmental Engineering, The Hong Kong Polytechnic University, Hong Kong
- ^c Department of Civil & Environmental Engineering, Imperial College London, London, UK

ARTICLE INFO

Keywords: Progressive collapse Retrofit Steel structures Robustness Load redistribution Dynamic response

ABSTRACT

A large proportion of the existing building stock has been designed without consideration for progressive collapse and may therefore need retrofitting. To this end, this study compares the performance of three typical retrofit strategies for existing multi-story steel-framed structures subjected to column loss scenarios. The strategies include global measures, such as horizontal bracings placed above the removal zone and a truss system added at the rooftop level, and a local measure based on strengthening the 1st story columns through concrete encasement. Five moment resisting frames, prone to different progressive collapse mechanisms, are considered for case study purposes. Detailed numerical models validated against experimental results are developed to investigate the robustness of the frames before and after retrofitting. Parametric non-linear static analyses are also conducted to optimize the design of the retrofit measures. Additionally, the study assesses the impact of retrofitting on the dynamic response through non-linear dynamic analyses. The results show that the effectiveness of retrofitting depends on several factors, including, most significantly, their ability to redistribute loads, the number of stories, and the type of collapse mechanism (e.g., failure of beams or columns). Moreover, it is shown that global measures have the most favorable influence on the dynamic behavior. The study reveals that no single strategy is effective across all configurations and that case-specific decisions are typically necessary, based on the vulnerabilities in each structure. The paper offers fundamental insights and practical considerations for designing and implementing the various retrofit measures, enabling more holistic and informed selection approaches.

1. Introduction

Accidental events, such as fires, explosions, or impacts, often cause localized damage to building structures, which may spread from element to element, leading to the partial or total collapse [1]. This behavior is known as progressive or disproportionate collapse, and despite its relatively low probability of occurrence, the potential consequences may be very high. Among others, disasters such as the collapse of the Ronan Point Building (London, 1968), the Murrah Federal Building (Oklahoma City, 1995), the World Trade Centre (New York, 2001), and more recently, the Champlain Towers (Miami, 2021), have shown the substantial social and economic losses that can arise from progressive collapse [2–5]. Progressive collapse mitigation is of utmost importance for structures where the three components that compose risk are highly prevalent. A large number of steel structures can be classified under this category. These are often designed with a low

level of redundancy and optimized sections for specific design actions (*i. e.*, high vulnerability), employed for large strategic or industrial buildings (*i. e.*, high consequence), and occupied by a large number of people or devoted to the provision of fundamental services (*i. e.*, high exposure). Non-structural protective actions, such as Hostile Vehicle Mitigation [6] or blast-resistant glazing measures, can be undertaken to limit the hazard. However, these measures are typically threat-dependent and effective against a single pre-identified type of hazard. Conversely, to mitigate the risk of progressive collapse against multiple threats, the focus has been on reducing the inherent vulnerability by designing 'robust' structures that can withstand local damage without suffering progressive collapse.

Significant progress has been made in recent years in understanding the mechanisms involved in progressive collapse [1–5,7–9], allowing the development of design codes and standards [10–12]. Nevertheless, code provisions incorporating detailed recommendations on progressive

E-mail address: f.freddi@ucl.ac.uk (F. Freddi).

^{*} Corresponding author.

collapse are relatively recent. For example, general requirements for robustness in new construction were first introduced in Europe in 2006 with the publication of Eurocode 1 Part 1–7 [10]. Over 220 million buildings in Europe (equivalent to 85 % of the building stock) were constructed before 2001, and 85–95 % of these buildings will likely still be standing in 2050 [13]. Currently, most existing structures were designed before the introduction of these provisions, hence without consideration for progressive collapse. A noteworthy example in the US is the 12-story Champlain Towers in Miami, which suffered from partial progressive collapse in 2021. The structure was completed in 1981, before the introduction of US recommendations against progressive collapse [11,12]. This highlights the need for advanced considerations regarding the robustness of the existing building stock and the definition of viable, effective, and sustainable retrofit strategies that can improve progressive collapse resistance.

Kiakojouri et al. [14] presented an extensive review of strengthening and retrofitting techniques for progressive collapse. For steel structures, most techniques focus on preventing the initial local damage [15,16]. In contrast, only a few research investigations [17-32] focused on enhancing the overall structural capacity. Global interventions were shown to be effective in several studies [17–28]. Astaneh-Asl et al. [17], Zhu et al. [18], and Papavasileiou and Pnevmatikos [19] showed that cables placed on each floor effectively increase redundancy and provide additional paths for the development of catenary actions. However, cables may require significant vertical displacements for their activation. Other studies focused on horizontal bracings spanning the whole width of the structure [20–22] and/or vertical bracings running from the bottom to the top of the structure [22-25], considering different positions, e.g., perimetral or internal spans, and various types of braces, including inverted V-bracing [23], X-bracing [24], and buckling restrained braces [25]. Horizontal bracing systems were shown to increase the capacity to withstand column removal scenarios by reducing the vertical displacements in the area above the removed column and redistributing vertical loads to the other columns. Vertical bracings exhibit a similar mechanism when placed above the removed column [23]. Conversely, when the removed column is in a different position, they act as strong boundaries, fostering larger catenary action in the beams [25] and limiting the extent of possible damage. Nevertheless, both cables and bracing systems may influence the structural dynamic behavior under horizontal actions, leading to potential detrimental effects on the structural performance under other actions (e.g., seismic response). Freddi et al. [26], Ferraioli et al. [27], and Mirvalad [26] investigated the use of a truss at the top of the structure (i.e., roof-truss) to facilitate load redistribution for horizontal bracings. This solution offers the advantage of increasing robustness while minimizing business interruption during implementation and having a minimal impact on the dynamic response. Nonetheless, the strength and stiffness of the rooftruss should be carefully calibrated to ensure an appropriate redistribution of vertical loads and avoid issues related to tension forces that may arise in the columns at higher levels.

In addition to the above, other solutions focused on enhancing the strength, stiffness, and/or ductility of beams, beam-column joints, or columns through local interventions [29–32]. Galal and El-Sawy [29] showed the effectiveness of strength and/or stiffness enhancements for beams. Liu [30] suggested the substitution of partial-strength shear-resisting joints with full-strength moment resisting alternatives to facilitate the development of catenary action. Similarly, Ghorbanzadeh et al. [31] investigated the use of duplex stainless-steel pins to enhance the strength and ductility of pinned joints. Gerasimidis and Banioto-poulos [32] considered an increased thickness of the plates forming the web of the columns as a strengthening technique, and suggested the addition of simple steel plates for retrofitting. It should be noted, however, that such local interventions typically entail lengthy business interruptions.

Although the above-discussed studies have proposed retrofit methods to enhance the overall performance against progressive

collapse, there is a need for a more systematic understanding of the benefits and limitations of retrofit solutions. Current research has primarily focused on isolated case studies, often overlooking the diverse mechanisms that govern the collapse of actual structures. For example, only a few studies have accounted for column buckling as a consequence of force redistribution. A more extensive assessment is therefore required, involving different framed configurations and not limited to preventing only ductile beam mechanisms. Strategies involving global or local interventions may effectively prevent progressive collapse for different collapse mechanisms. Bracing or roof-truss systems are global interventions that may be designed to facilitate significant load redistributions. Conversely, improved column capacity is typically addressed with local interventions, such as column encasement. Only a few studies have examined the comparative effectiveness of these global and local strategies to assess their respective merits; hence, additional research is needed in this direction. The present study advances research in this area by comparing different retrofit strategies and their effectiveness in mitigating the development of various failure mechanisms in steel-framed structures (e.g., beam failure, column buckling). The paper offers several insights into key aspects of the retrofit measures, including their impact on the redistribution of vertical loads and the dynamic response of the steel frames. Additionally, fundamental considerations for the practical implementation of these measures are provided. Moreover, this study assesses the potential deployment of coupled retrofit strategies, comparing the effectiveness of such an approach with alternatives based on a single measure.

This study comparatively examines the effectiveness of three different retrofit strategies for steel structures. Global solutions capable of redistributing vertical loads and retaining vertical displacements, namely bracing and roof-truss systems, are explored. A local intervention to enhance column capacity through column encasement is also considered. The assessment focuses on five case study steel Moment Resisting Frames (MRFs) varying from low- to high-rise. Non-linear Finite Element (FE) models are developed in OpenSees [33], with particular attention to possible failure modes that may arise from progressive collapse scenarios, such as combined catenary and bending actions at the joints and buckling in the columns. The effects of design parameters and optimal configurations that ensure robustness while minimizing material usage are identified through parametric analyses. The loss of the central 1st story column is simulated, focusing on a scenario maximizing the risk [26,34-42]. Non-linear static analyses are carried out, accounting for dynamic effects using the Dynamic Increase Factor (DIF). Additionally, a procedure involving dynamic analyses is employed to assess the impact of retrofitting on the dynamic effects resulting from column removal.

2. Structural configurations and modeling procedures

This section describes the configurations of the case study steel MRFs and the FE modeling in OpenSees [33]. The structures were selected to examine the performance of typical existing MRFs under the central column removal scenario and evaluate the effectiveness of different retrofit approaches.

2.1. Framed structures

Fig. 1 shows the layout of the five steel MRFs selected for case study purposes. These MRFs have been previously investigated by Gerasimidis et al. [40] and considered sensitive to progressive collapse. The design was performed in accordance with the Eurocodes [43–45]. The structures were assumed to be located in Greece; hence, the design accounted for the seismic load, considering a horizontal peak ground acceleration of 0.16 g. The frames have story heights of 3 m and total heights of 9, 18, 27, 36, and 45 m for the 3-, 6-, 9-, 12-, and 15-story structures, respectively. The frames consist of 4 bays of 6 m for the 3- and 6-story structures and 5 m for the 9-, 12-, and 15-story structures. A bay span

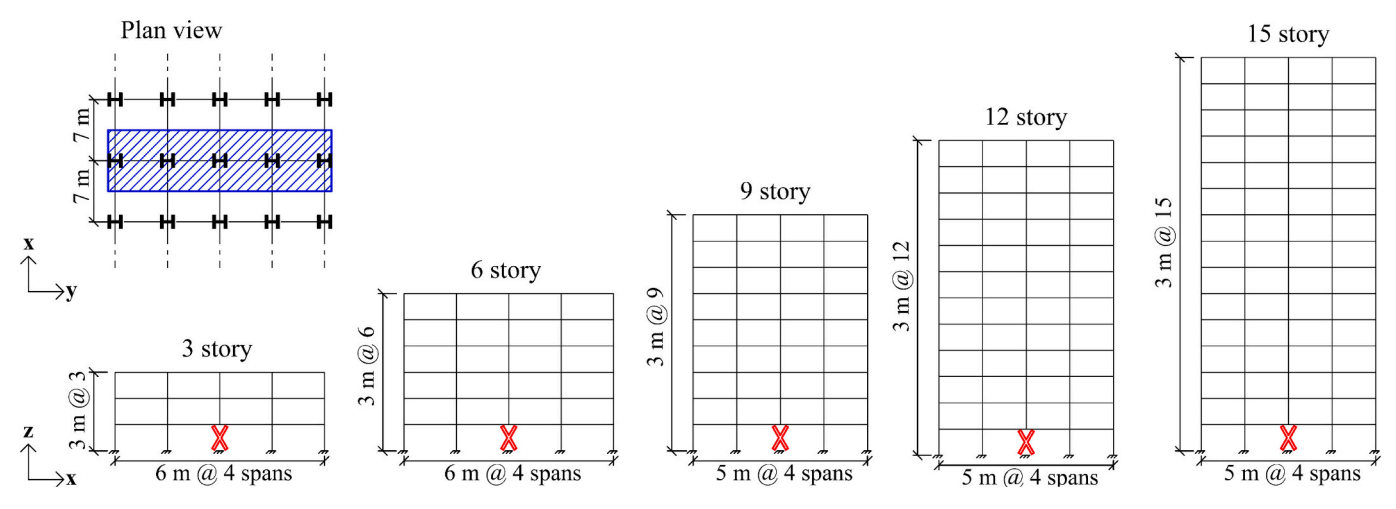


Fig. 1. Configuration of selected steel moment resisting frames (MRFs). (Adapted from Gerasimidis et al. [40]).

in the transversal direction of 7 m was considered. The steel sections were oriented with their major axis parallel to the frame plane, and the beam-column joints were designed as rigid, full-strength welded connections. The steel cross-sections for columns and beams are summarized in Table 1. All steel elements and components were made of steel of Grade \$235.

A Dead Load (DL) of $5.0~kN/m^2$ was applied to all floors, *i.e.*, $3.0~kN/m^2$ of self-weight for a 120 mm thick concrete slab plus $2.0~kN/m^2$ of non-structural permanent load. DLs were also applied directly to the beams and columns to consider their self-weight. A Live Load (LL) of $2.0~kN/m^2$ was applied to all floors below the roof level. The Snow Load (SL) on the roof was assumed to be $0.69~kN/m^2$, according to Eurocode guidelines [45] for the Greek climate region in Zone III, at an altitude of 200~m and under standard conditions. The load combination selected to assess the progressive collapse resistance was determined according to UFC [11], as follows:

$$q_d = 1.2 DL + (0.5 LL \text{ or } 0.2 SL)$$
 (1)

Table 1 also presents the Work Ratio (WR) of the ground story columns under the load combination in Eq. (1). The WR was computed as the ratio between the axial force N and the buckling resistance about the weak axis $N_{b,Rd}$, in accordance with EN1993-1-1 [43].

2.2. Finite Element (FE) modeling

3D FE models of the case-study plane MRFs were developed in OpenSees [33]. Fig. 2 summarizes the modeling strategy using the 9story MRF for illustration purposes, with Fig. 2(b), (c), and (d) showing the modeling approaches adopted for beams, columns, and joints, respectively. Beams were modeled with a lumped plasticity approach, while columns were modeled with a distributed plasticity approach to account for the interaction between axial forces and bending moments. Preliminary analyses indicated that discretizing beams and columns into 6 elements was sufficient to accurately capture their response. Fig. 2(a) also shows the position of masses included in the model when detailed dynamic analyses are performed (see Section 5.3). The column bases were fixed in the in-plane direction and hinged in the out-of-plane direction. Additional lateral restraints were incorporated at each floor at the beam-column joints in the out-of-plane direction. These restraints were introduced to prevent a global out-ofplane loss of stability and to consider the lateral stiffness of the slab and frames in this direction.

Beams were modeled as 'elasticBeamColumn' elements. The plastic hinges at the beam ends were implemented through the 'Parallel Plastic Hinge' (PPH) model (Fig. 2(b)) proposed by Lee et al. [46]. The PPH

Table 1
Case studies MRFs: columns and beam design. (Adapted from Gerasimidis et al. [40]).

N. of stories	Structural scheme	Columns		Ground story	column Work r	atio (WR) [%]		Beams
			Col 1	Col 2	Col 3	Col 4	Col 5	
3	6 m span, 3 m height	HE280B story 1 to 3	14.75 %	33.75 %	31.86 %	33.72 %	14.96 %	IPE500 story 1
								IPE400 story 2
								IPE360 story 3
6	6 m span, 3 m height	HE320B story 1 to 3	24.55 %	54.81 %	52.58 %	54.73 %	25.11 %	IPE550 story 1
		HE220B story 4 to 6						IPE450 story 2 to 3
								IPE400 story 4 to 6
								IPE360 story 6
9	5 m span, 3 m height	HE400B story 1 to 3	25.98 %	53.02 %	53.43 %	52.91 %	26.87 %	IPE550 story 1
		HE280B story 4 to 6						IPE500 story 2 to 3
		HE220B story 7 to 9						IPE450 story 4 to 6
								IPE400 story 7 to 8
								IPE360 story 9
12	5 m span, 3 m height	HE500B story 1 to 3	30.25 %	57.75 %	59.70 %	57.66 %	31.49 %	IPE550 story 1
		HE340B story 4 to 6						IPE500 story 2 to 6
		HE280B story 7 to 9						IPE450 story 7 to 9
		HE200B story 10 to 12						IPE360 story 10 to 12
15	5 m span, 3 m height	HE650B story 1 to 3	33.79 %	59.38 %	62.79 %	59.36 %	35.33 %	IPE550 story 1 to 2
		HE450B story 4 to 6						IPE500 story 3 to 9
		HE340B story 7 to 9						IPE450 story 10 to 12
		HE280B story 10 to 12						IPE500 story 13 to 14
		HE200B story 12 to 15						IPE450 story 15

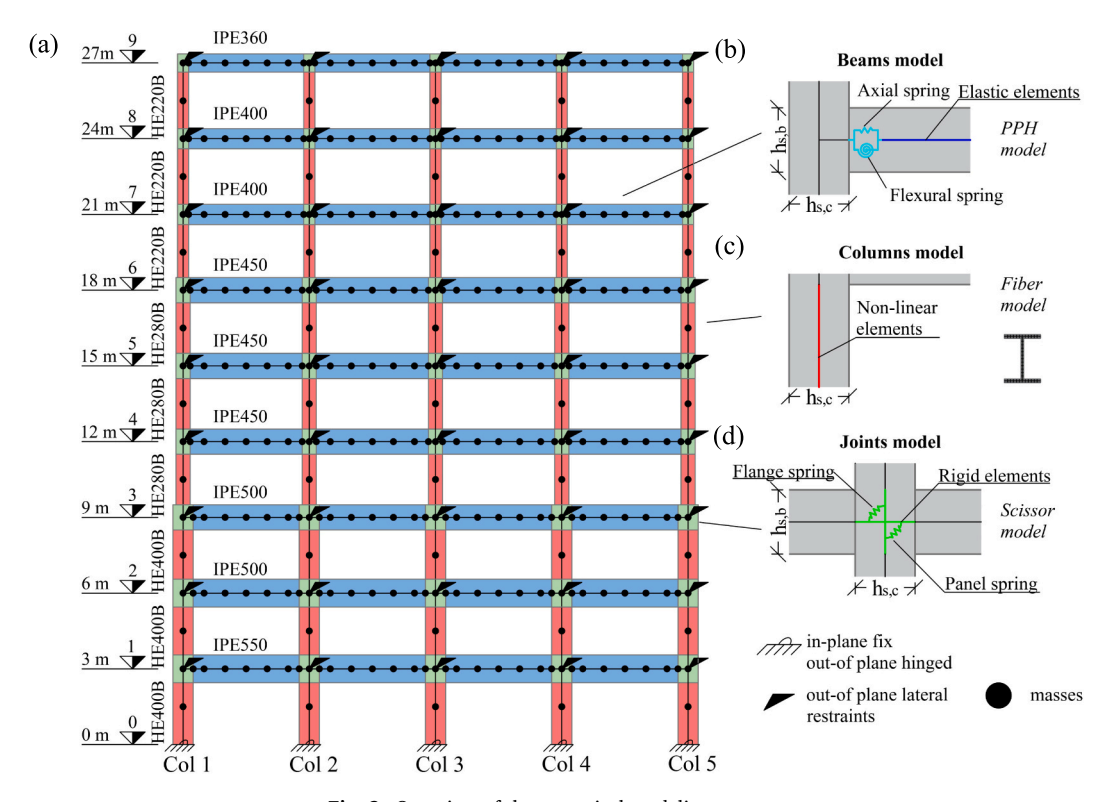


Fig. 2. Overview of the numerical modeling strategy.

consists of two 'zeroLength' springs, with flexural and axial behavior, and allows for capturing the bending moment and axial force interactions. This is particularly important when simulating progressive collapse scenarios due to the large contribution provided by the catenary actions. The PPH model was validated against the experimental results by Dinu et al. [47], and model parameters were then derived for the beams of the case-study MRFs. Details of the validation procedure can be found in Possidente et al. [42].

Columns were modeled as 'ForceBeamColumn' elements (Fig. 2(c)), which account for both material and geometric non-linearities. The fibers were modeled using the 'Steel01' material with yield strength $f_y = 235$ MPa, Young's modulus E = 210,000 MPa, and a 0.2 % post-yield stiffness ratio. The elastic contribution of shear stiffness was included through the 'Section Aggregator' while both the in- and out-of-plane buckling were modeled by introducing local and global equivalent imperfections according to the EN 1993-1-1 [43] recommendations. In detail, for each column, an initial local bow imperfection with magnitude e_0 was defined according to Table 5.1 of EN 1993-1-1 [43], considering the values for plastic analysis. The magnitude of the initial sway imperfection was defined through the initial rotation ϕ , as follows:

$$\phi = \phi_0 \alpha_h \alpha_m \tag{2}$$

where $\varphi_0=1/200$ is the basic rotation value, and α_h and α_m are the reduction factors to account for the height of the structure and the number of sufficiently stressed columns in a row, respectively.

Beam-column joints were modeled through the 'Scissor Model' [48] (Fig. 2(d)), whose main parameters were determined according to Charney and Downs [49]. This model uses two rotational 'zeroLength' springs to account for the deformability of the column web panel and flanges. The springs were connected to two orthogonal 'elasticBeamColumn' rigid elements, whose extension is consistent with the physical dimensions of the joints.

The 'Corotational' formulation was employed for all elements to simulate the effects occurring with large displacement, such as catenary action. Loads were uniformly distributed along the beams. Additional

modeling information affecting the dynamic response is provided in subsequent relevant sections.

The present study considers several modeling simplifications. As a conventional solution, e.g., [26,32,40–42,50], it considers single MRFs, disregarding the possible positive contributions from other components, such as the slab and the transverse beams. This is a conservative choice, and among others, it is justified by the fact that, in existing structures, the slab may not be composite, and limited information may be available to estimate its contribution. Lateral-torsional buckling was also neglected; however, it was checked a posteriori, confirming that this simplification did not affect the results. In the present study, column bases are assumed to be fixed in the in-plane direction. To more accurately capture the structural response and buckling resistance of the first-story columns, more refined and case-specific models could incorporate the actual rotational stiffness of the base connections.

3. Assessment of existing frames

The robustness of the existing structures is assessed using the Alternate Path Method (APM), considering the loss of the central column at the 1st story. The numerical procedures are first outlined, and the results are then presented and discussed, with an emphasis on the mechanisms that lead to collapse.

3.1. Numerical procedure

The APM is applied in a three-step static procedure, as illustrated in Fig. 3:

In Step 1, a 'gravity analysis' is performed for the existing structure by applying the loads defined for the relevant load combination (Eq. (1)). This step assesses the state of the undamaged structure immediately prior to the removal event. In this step, the force R_3 acting on the central column is determined.

In Step 2, namely the 'state restoring phase', the damaged structure, *i. e.*, without the central column, is assessed. In this step, the state before removal is restored by performing a gravity analysis in a model where

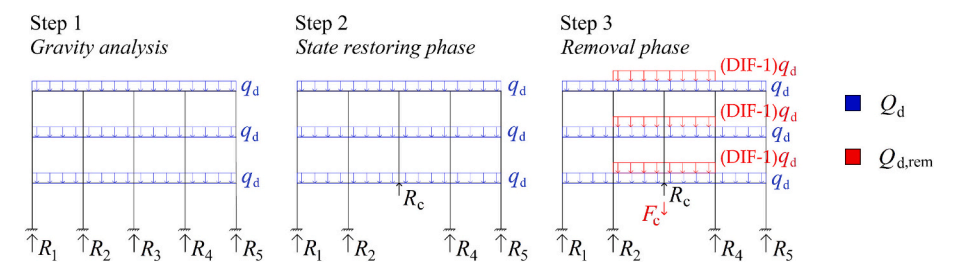


Fig. 3. Procedure for non-linear static analyses.

the column is removed and replaced by a force R_c equal to the force R_3 measured in the previous step. Although, in principle, the actions associated with each degree of freedom should be considered to replace the removed column, previous research showed that neglecting the contribution of shear and bending moments leads to negligible differences [26].

In Step 3, namely the 'removal phase', the progressive collapse is simulated. The effect of the column removal is simulated by statically increasing a concentrated load equal and opposite to $R_{\rm c}$ ($F_{\rm c}$ in Fig. 3). In addition, as a static analysis is carried out, the distributed loads $q_{\rm d}$ in the adjacent beams above the removal are amplified with the DIF to account for dynamic effects indirectly. In this study, the DIF values were determined according to UFC 4–023 [11] as a function of the target structural response level and expected ductility demand of beam elements. Considering welded unreinforced flange connections, which ensure a plastic rotation angle of $\theta_{\rm pra}=0.0284$ –0.0004 h, where h is the beam depth, the following DIF values were obtained: 1.27 for the 3- and 6-story MRFs, 1.24 for the 9- and 12-story MRFs, and 1.22 for the 15-story MRF.

The application of the loads throughout the phases involving the damaged structure, *i.e.*, the *state restoring* and the *removal phases*, is monitored by the load factor λ , defined as follows:

$$\lambda = \frac{\sum_{i=1}^{n} R_i}{Q_{tx}} \tag{3}$$

where $\sum_{i=1}^{n} R_i$ is the sum of the vertical base reaction forces of the frame, and Q_{tg} is the load target the structure is supposed to bear according to the load combination, *i.e.*, the target demand. In particular, Q_{tg} can be split into two terms: i) the downward loads Q_{d} applied during the *state restoring phase* (in blue in Fig. 3), and ii) the additional downwards loads $Q_{d,rem}$ applied during the *removal phase*, consisting of the load increment to account for dynamic effects in the area above the removed column and the force F_c (in red in Fig. 3).

$$Q_{\rm tg} = Q_{\rm d} + Q_{\rm d,rem} \tag{4}$$

Failure is observed when the loads cannot be further increased during the *removal phase*. If failure is detected for $\lambda < 1$, the structure is unable to withstand the target load and is prone to progressive collapse. Conversely, if failure occurs for $\lambda > 1$, the structure can withstand the target demand and retain residual bearing capacity.

3.2. Progressive collapse evaluation

Fig. 4 shows the results of the progressive collapse analyses (*i.e.*, Steps 2 and 3) for the five case study structures in terms of the load factor λ vs. the vertical displacement δ above the removed column. An increase in displacement δ occurs during the removal phase, *i.e.*, Step 3, when the removal force F_c and the loads accounting for dynamic effects are applied. The displacement δ increases significantly in the 3- and 6-story MRFs in which a beam mechanism, *i.e.*, the formation of plastic hinges in the beams' ends, develops, eventually leading to failure. Conversely, a much lower displacement δ is measured at collapse in the 9-, 12-, and 15-story structures. In these cases, collapse occurs due to a column

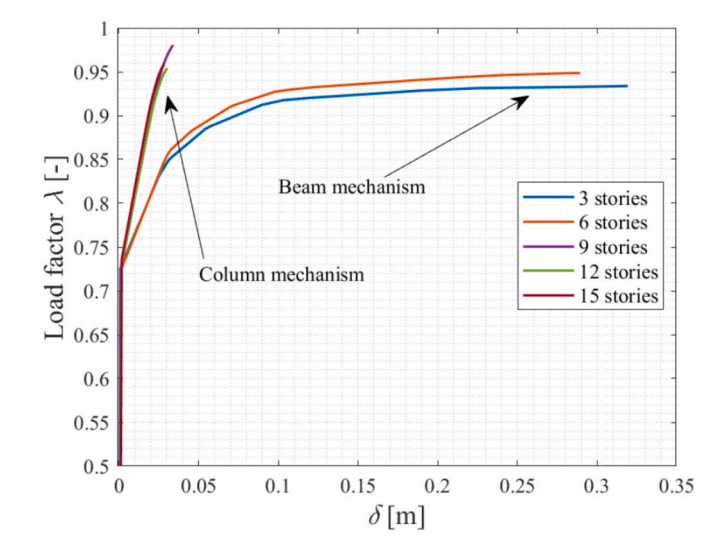


Fig. 4. Load factor evolution for existing structures.

mechanism, i.e., buckling in the 1st story columns.

The typical behavior of structures in which one of the two mechanisms is predominant is better described in Fig. 5. Fig. 5(a) shows the deformed configuration at collapse of the 3-story MRF, highlighting the beam mechanism. Here, the maximum bending moment $M_{\rm m}$ has been attained at all beam ends of the central spans at the 1st (red lines), 2nd (blue lines), and 3rd story (green lines). Large rotations allow for the formation of plastic hinges, which preclude any further load increase and cause the collapse of the central part of the structure.

Similarly, Fig. 5(b) shows the deformed configuration at collapse for the 12-story MRF, in which out-of-plane buckling occurs in the two internal columns at the 1st story, i.e., Column 2 (light blue lines) and Column 4 (orange lines). In these columns, the axial load N approaches the buckling resistance $N_{\rm b}$, and out-of-plane runaway displacements u_y are measured at the mid-length of the columns. Collapse occurs when the structure cannot redistribute the loads acting on the buckled columns to the other elements.

Table 2 reports the failure mechanisms and maximum load factors attained for each MRF. In general, none of the structures can withstand the progressive collapse scenario, as the load factors measured at collapse are lower than one. It should be noted that the buckling resistance $N_{\rm b}$ of the critical columns at the 1st story was evaluated numerically to account for the influence of the stiffness of the remainder of the structure. An additional downward load was applied to the critical columns in the models of the damaged frames (*i.e.*, without the central column) subjected to gravity loads. The maximum axial force measured in the critical columns was assumed as the buckling resistance $N_{\rm b}$. The $N_{\rm b}$ values obtained for each MRF are provided in Table 2.

4. Design and performance of retrofitted structures

This section deals with the design of the three retrofit solutions

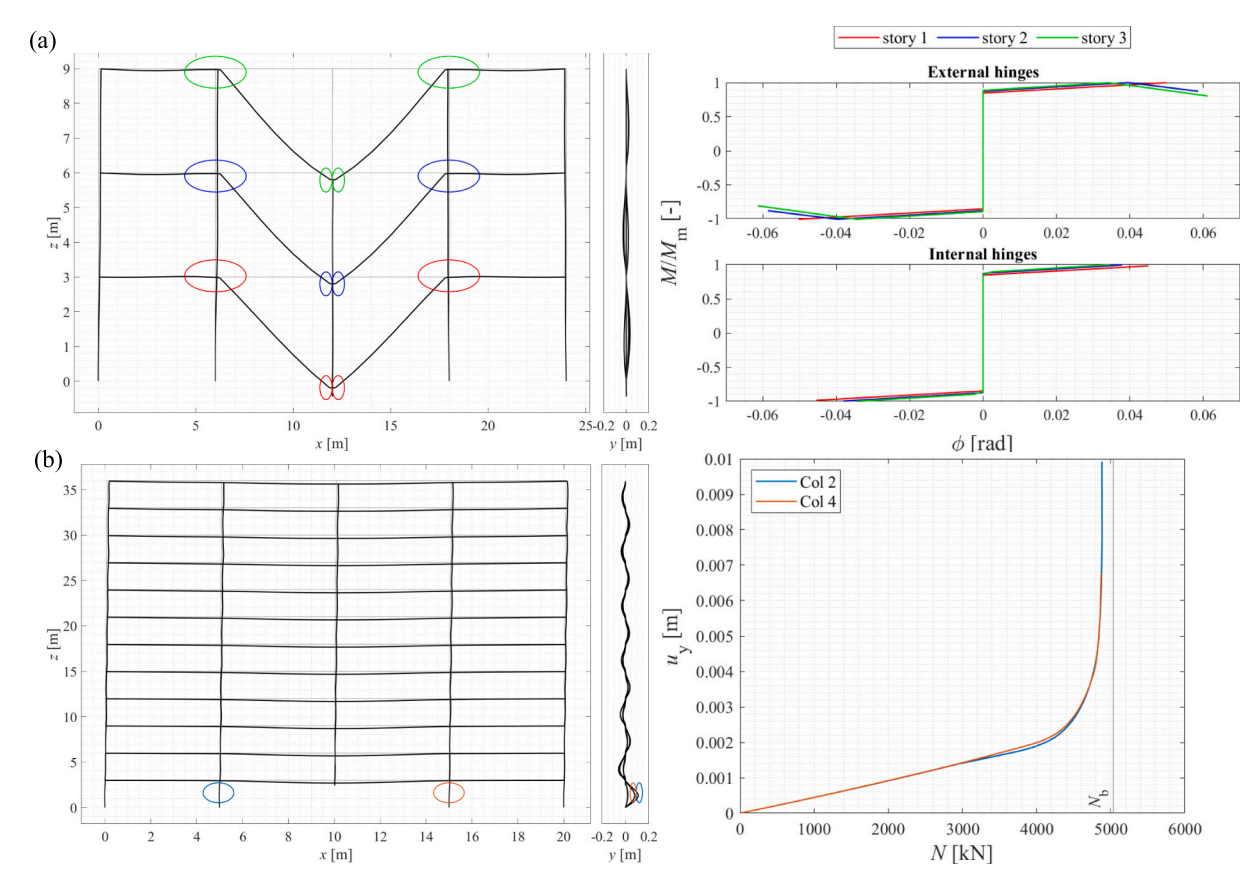


Fig. 5. Deformed configuration at collapse ($10\times$) and governing mechanism: (a) 3-story MRF; (b) 12-story MRF.

 Table 2

 Capacities and failure mechanisms of the existing structures.

N. of stories	Load factor (λ_{\max})	Failure mechanism	N _b 1st story columns [kN]
3	0.93	Beam	2633
6	0.95	Beam	3279
9	0.98	Column	4078
12	0.95	Column	5036
15	0.96	Column	6002

depicted in Fig. 6. Parametric analyses are conducted to optimize the design and examine the effectiveness of the various solutions. The results for the 3- and 12-story structures are discussed in detail to illustrate

key aspects of the response.

4.1. Retrofit measures

The first retrofit measure, illustrated in Fig. 6(a), involves a bracing (BR) system with diagonal members installed at the 2nd story. The location of the system was selected to effectively tackle only the 1st story column loss scenario with minimal modification to the original structural properties. By enhancing the redistribution capacity, the bracing system transfers the loads previously carried by the removed column to the undamaged columns. Circular diagonal braces were considered and implemented within the FE models, including initial imperfections according to EN 1993–1–1 and employing 'ForceBeamColumn' elements [33]. The ends of the braces were connected through internal hinges to

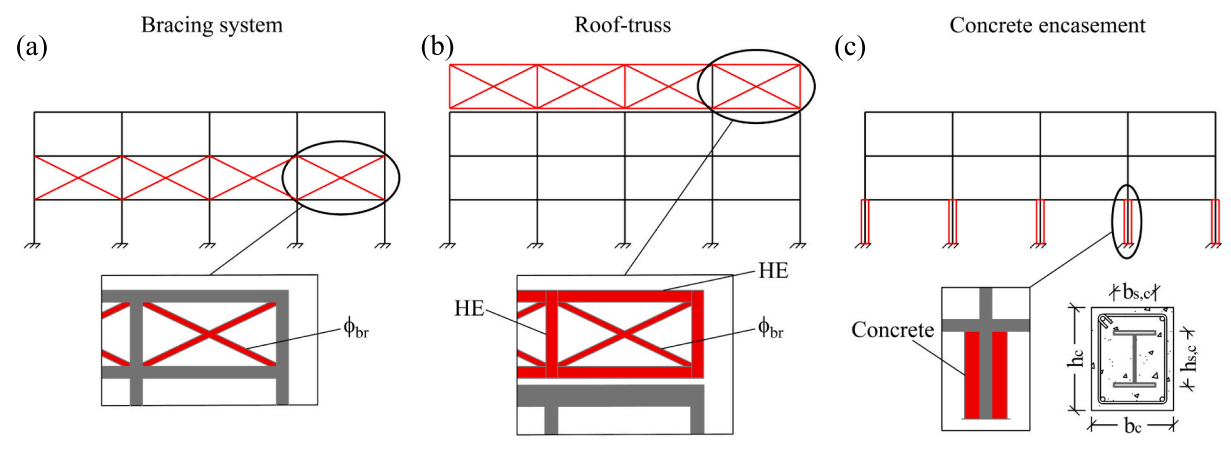


Fig. 6. Investigated retrofit strategies: (a) Bracing system; (b) Roof-truss; (c) Column encasement.

rigid diagonal elements, simulating the dimensions of the steel sections in the beam-column connection zones. Braces were made of steel S355 with a yield strength $f_{\rm y}=355$ MPa and Young's modulus $E=210{,}000$ MPa.

The second retrofit measure, illustrated in Fig. 6(b), involves a truss system placed at the top of the structure, *i.e.*, 'roof-truss' (RF), connected to all column ends of the top story. Similar to the bracing system, the 'roof-truss' aims at redistributing loads to the undamaged columns. However, unlike the bracing system, due to its location, this retrofit solution effectively tackles column loss scenarios at different levels. Circular diagonal braces were considered and modeled using the same strategy employed for the BR system. Internal hinges were considered between the braces and the rigid diagonal elements, simulating the dimensions of the steel sections in the beam-column connection zones. HE sections were considered for vertical and horizontal members, which were modeled with 'ForceBeamColumn' elements [33] to account for the possible spread of plasticity. All components were made of steel S355 with a yield strength $f_y = 355$ MPa and Young's modulus E = 210,000 MPa.

The third retrofit measure, illustrated in Fig. 6(c), involves concrete encasement (EN) of steel columns. The encasement is applied to all the columns of the 1st story. This solution could also be applied to selected stories at higher levels, depending on the case. The main scope of column encasement is to prevent buckling of the steel section. A further beneficial effect is the protection of the columns from threats such as fires, impact, and explosions. The encasement was modeled with 'ForceBeamColumn' elements. The initial design consisted of the minimum dimensions to comply with the recommendations of Eurocodes [44,51,52] and, therefore, was sized for the specific steel columns. Relevant design dimensions are depicted in Fig. 6(c). The 'Concrete01' material model in OpenSees was used for the encasement. The use of this model implies the conservative assumption that concrete makes no contribution to tension. Concrete Grade C25/30 with $f_{\rm cm}=33$ MPa and steel rebars with $f_{\rm V,rb}=450$ MPa were considered.

The three retrofit measures were selected to explore the effectiveness of solutions conceived for different situations. The roof-truss system is an additional structure that enhances the robustness and redundancy of the building, allowing for more alternative load paths. This strategy is primarily effective against beam mechanisms; however, in some cases, its strength and stiffness can be calibrated to enhance the load redistribution and delay the onset of the column mechanisms. Conversely, the column encasement directly improves the capacity of the columns and is, therefore, a specific case-based solution, suited only for column mechanisms. The bracing system is somehow in between, as it is conceived to mitigate the removal of a column at or below a specific story.

State restoring phase Removal phase Q_{d,rem}/Q_{tg} Q_{d,rem}/Q_{tg} Page 1 O.7 V. 0.6 O.9 O.1 O.1 O.1 O.2 Step 2 Step 3 (a)

4.2. Analysis procedure

A procedure similar to that described in Section 3.1 is used to analyze the retrofitted structures. Step 3 of the analysis remains unchanged, while Steps 1 and 2 are split into two sub-steps to account for the installation of the retrofit measures.

In Step 1, a 'gravity analysis' is performed first on the existing undamaged structure by applying the loads defined for the relevant load combination and providing the base reaction $R_{\rm c}$ (Step 1a). Once equilibrium is reached, the retrofit measure is introduced in the model, and its loads are applied to the retrofitted structure. The new base reaction force $R_{\rm c,tot}$ is obtained, and the contribution of the retrofit system to the base reaction force is then determined as $R_{\rm c,ret} = R_{\rm c,tot} \cdot R_{\rm c}$ (Step 1b).

In Step 2, the 'state restoring phase' is modified to account for the implementation of the retrofit strategy in a similar way to Step 1. Step 2a simultaneously applies the gravity loads and the reaction force $R_{\rm c}$. This step is shown in blue in Fig. 7(b) and is equivalent to Step 2 in the case of the existing MRF in Fig. 7(a). Step 2b implements the retrofit system, its loads $Q_{\rm d,ret}$, and the additional contribution to the reaction force $R_{\rm c,ret}$. This step is specific to the case of the retrofitted structures and is shown in the green region in Fig. 7(b).

In Step 3, the 'removal phase' remains unchanged, as shown in the red region in Fig. 7(b), and the full reaction force $R_{\rm c,tot}$, and load amplification through the DIF are considered.

Hence, in the case of the retrofitted MRFs, the target load consists of the following three terms:

$$Q_{tg} = Q_{d} + Q_{d,ret} + Q_{d,rem}$$
 (5)

4.3. Bracing system (BR)

For the bracing system, the brace diameter $\phi_{\rm br}$ was varied, with increments of 20 mm to identify the optimal configuration.

Fig. 8(a) shows the evolution of the load factor against the displacement above the removal for the 3-story MRF. In this case, the bracing system is effective ($\lambda \geq 1$), and the parametric analysis led to identifying $\phi_{br} = 40$ mm as the optimal design. Interestingly, for $\phi_{br} \leq 60$ mm, collapse occurs at large displacements δ for the development of the beam mechanism, whereas for $\phi_{br} \geq 80$ mm, collapse occurs at smaller displacements δ for the buckling of the 1st story columns, due to the higher loads transferred by the bracing systems with increased strength/stiffness. Further increasing the diameter ϕ_{br} does not provide any benefit to the columns. These considerations are summarized by the insets in Fig. 8(a). Here and in the following analogous figures, the performance of the frame is shown in terms of maximum load factor λ with respect to the increase in design variables, i.e., the diameter ϕ_{br} .

Fig. 8(b) shows similar plots for the 12-story MRF. In this case, the bracing system is ineffective (λ < 1), regardless of the brace diameter

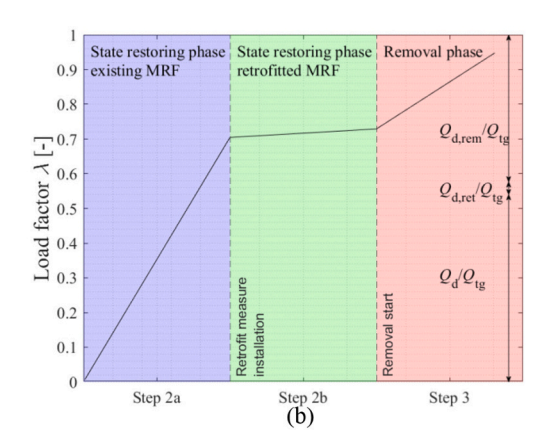
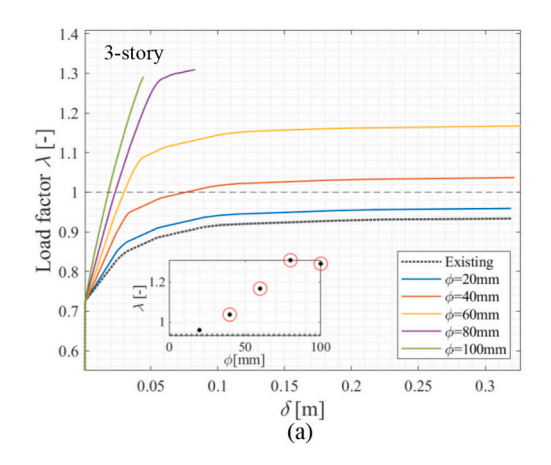


Fig. 7. Load application phases for: (a) existing and (b) retrofitted structures.



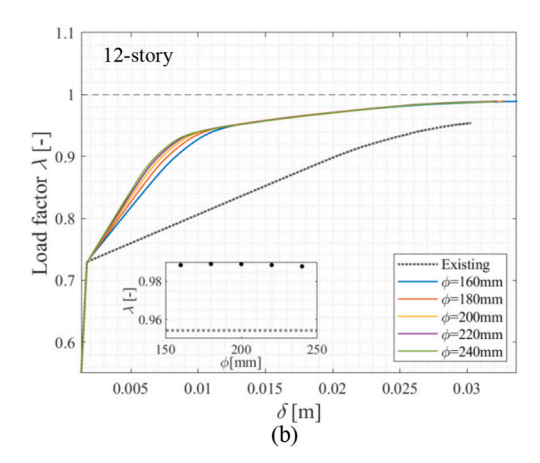


Fig. 8. Bracing system response: (a) 3-story MRF; (b) 12-story MRF.

 $\phi_{\rm br}$. The bracing system provides a significantly stiffer response to the structure, *i.e.*, more than twice as stiff as the existing frame; however, the development of the column mechanism prevents it from reaching $\lambda \geq 1$. Again, further increasing the diameter $\phi_{\rm br}$ does not provide any benefit to the columns.

4.4. Roof-truss (RT)

For the roof-truss, the diameter of the braces $\phi_{\rm br}$ was varied, considering increments of 20 mm as for the bracing system above. The initial design assumption for the horizontal and vertical members considered HE400M sections and a roof-truss height equivalent to the inter-story height of the structures, *i.e.*, $H_{\rm RF}=3$ m. This design was based on a previous study in which various dimensions and sections for the vertical and horizontal elements were considered [26]. The sections and the height $H_{\rm RF}$ were also varied to calibrate the strength and stiffness of the roof-truss and find the optimal solution.

Fig. 9(a) shows the evolution of the load factor with the displacement δ for the 3-story MRF. The roof-truss is effective ($\lambda \geq 1$), and the optimal design is identified for horizontal and vertical members with HE260M sections, a height $H_{RF}=1$ m, and a diameter of the braces $\phi_{br}=20$ mm. For $\phi_{br}=20$ mm, collapse occurs at large displacements δ and is reached due to the development of the beam mechanism, with plastic hinges also forming in the horizontal elements of the roof-truss. For $\phi_{br}\geq 20$ mm, collapse occurs at smaller displacements δ and is due to the buckling of the 1st story columns. Further increasing the diameter ϕ_{br} may become detrimental if excessive axial loads are transferred to the columns, making them critical for lower load factors. Compared to the bracing system, the roof-truss allows for a more significant increase in the load

factor.

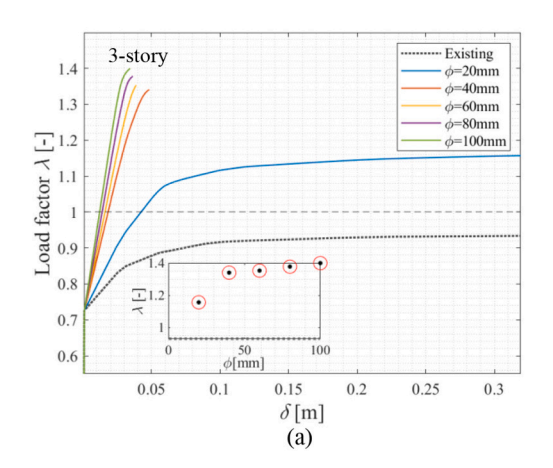
Fig. 9(b) shows similar plots for the 12-story MRF. The roof-truss is effective ($\lambda \geq 1$), and the optimal design is identified for horizontal and vertical members with HE600M sections, a height $H_{RF}=3$ m, and a diameter of the braces $\phi_{br}=100$ mm. Regardless of the diameter of the braces ϕ_{br} , the maximum load factor is achieved with the MRF developing the column mechanism. Increasing the diameter of the braces provides a minimal performance increase, as they have little influence on the redistribution of vertical loads to the columns.

The calibration of vertical and horizontal members, as well as the height HRF, was crucial in determining an optimized design for the roof-truss. Indeed, the initial design assumptions, *i.e.*, HE400M sections and $H_{RF}=3$ m, were modified in the two cases shown in Fig. 9. For the 3-story MRF, an effective roof-truss could be designed based on the initial design assumptions. However, reducing the steel sections and the height H_{RF} enabled a better exploitation of the steel sections while using less material. Conversely, for the 12-story MRF, the initial design did not ensure sufficient redistribution of the vertical loads to the perimeter columns, and the internal columns became critical for load factors $\lambda < 1$. The modified design led to an increase in the stiffness of the roof-truss, thus ensuring a more uniform load redistribution across the 1st story columns.

4.5. Column encasement (EN)

For encased columns, the encasement depth b_c and height h_c (see Fig. 6) were varied considering increments of 50 mm, starting from the minimum design complying with Eurocodes [44,51,52].

Fig. 10(a) shows the evolution of the load factor against the



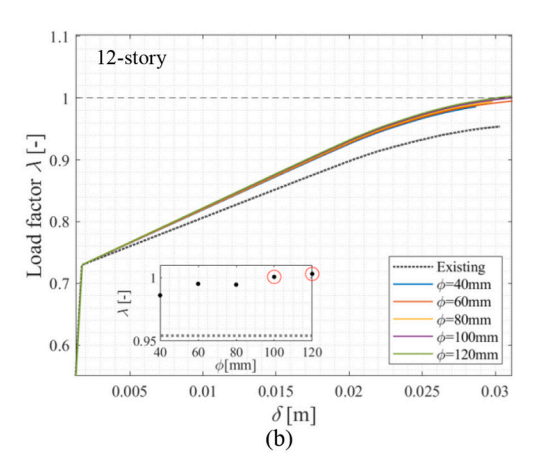
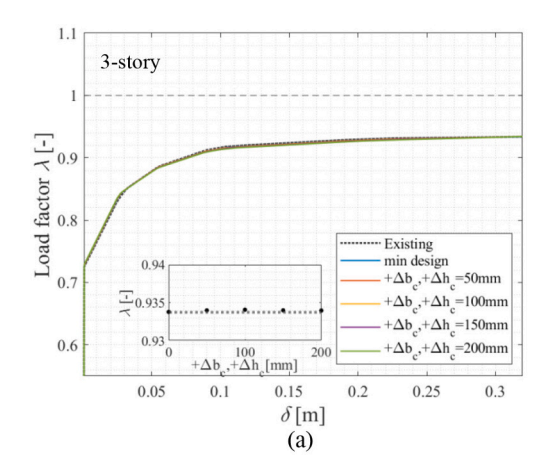


Fig. 9. Roof-truss assessment: (a) 3-story MRF, $H_{RF}=1$ m and HE260M; (b) 12-story MRF, $H_{RF}=3$ m and HE600M.



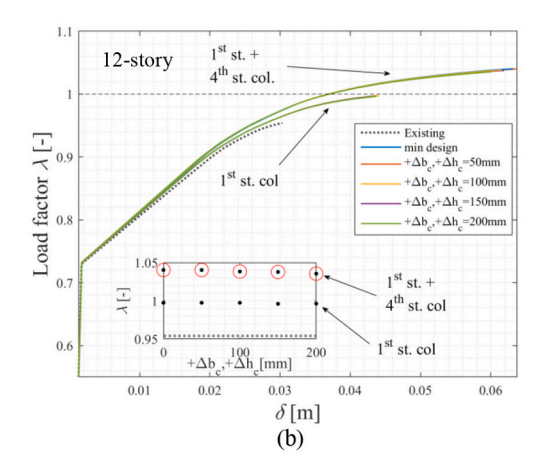


Fig. 10. Encased column assessment: (a) 3-story MRF with 1st story columns encasement; (b) 12-story MRFs with 1st story columns encasement and both 1st and 4th story columns encasement.

displacement above the removed column for the 3-story MRF. The encasement of the columns at the 1st story is shown to be ineffective (λ < 1), regardless of the design. As expected, the column encasement cannot increase the structural performance to λ > 1, as a beam mechanism governs the collapse scenarios. Increasing the encasement dimensions provides no benefits, and the response of the MRF considering different configurations is essentially superimposed.

Fig. 10(b) shows similar plots for the 12-story MRF. The encasement of the columns at the 1st story increases the capacity of the MRF and can be deemed successful as λ is very close to one, within the 0.996–0.997 range. Increasing the dimensions of the encasement has no effect, as column buckling at the 1st story is effectively prevented already with the minimum design.

It is worth noting, as indicated in Fig. 10(b), that with the encasement of the columns at the 1st story, $\lambda \geq 1$ cannot be reached because other structural elements become critical. Indeed, as the retrofitted MRF accommodates higher loads, buckling in the internal columns eventually appears at the 4th story. Fig. 10(b) shows that an additional configuration with column encasement introduced at both the 1st and 4th story levels further enhances the overall performance, leading to improved performance ($\lambda \geq 1$). As a general feature of this measure, increasing the size of the concrete envelope at the 4th level does not provide any load factor increase but instead shows a slight negative effect due to increased loads.

5. Effectiveness of retrofit strategies

This section presents the main findings from the numerical simulations and discusses the effectiveness of the retrofit measures. The benefits and drawbacks of each strategy, including their redistribution capacity and dynamic response, are investigated and compared, providing insights into their performance and practical implementation.

5.1. Overall performance

Table 3 summarizes the main results of the progressive collapse analyses performed on the five retrofitted MRFs.

The 3-story MRF was successfully retrofitted ($\lambda_{max}>1$) with the bracing system and the roof-truss. The optimized design of these measures used small braces and sections. The encasement could not provide any improvement to the progressive collapse resistance. The failure at λ_{max} is characterized by the beam mechanism for all cases.

The 6-story MRF was successfully retrofitted ($\lambda_{\rm max}>1$) only with the roof-truss. The optimized design of this measure features larger braces and sections compared to the 3-story MRF, enabling a more effective redistribution of loads to the perimeter columns. The implementation of the roof-truss generates a switch in the failure mode at $\lambda_{\rm max}$. The failure transitions from the beam mechanism of the existing frame to the column mechanism at the 1st story columns. With the bracing system, collapse at $\lambda_{\rm max}$ occurred due to the beam mechanism for small braces and the column mechanism with larger braces, but always with $\lambda_{\rm max}<1$. Again, the encasement did not provide any improvement to the

Table 3Comparison of retrofit effectiveness.

N. of stories	Load factor (λ_{max})			Optimal design variable			Collapse mechanism at λ_{max}				
	EX	BR	RF	EN	BR $\phi_{\rm br}$ [mm]	RF^a $\phi_{ m br}$ [mm]	$ ext{EN}^{ ext{b}} \ ext{b}_{ ext{c}} imes ext{h}_{ ext{c}} ext{ [mm}^2]; ext{n}_{ ext{l}} imes ext{\phi}_{ ext{l}} ext{ [mm]}$	EX	BR	RF	EN
3	0.93	1.04	1.16	<1	40	20	_	Beam	Beam	Beam	Beam
6	0.95	<1	1.01	<1	_	80	_	Beam	Beam/Col. 1st st	Col. 1st st	Beam
9	0.98	<1°	1.01	1.05	-	40	410 × 510	Col. 1st st	Col. 1st st	Col. 1st st	Col. 4th st
12	0.95	<1	1.00	1.04	-	100	8×18 at 1st st. 420×620 8×20 at 1st st. +	Col. 1st st	Col. 1st st	Col. 1st st	Col. 2nd st
15	0.96	<1°	<1	1.01	-	-	410×450 8 × 18 at 4th st. 450×800 8 × 24 at 1st st.	Col. 1st st.	Col. 1st st.	Col. 1st st	Col. 4th st

^a Additional design details: H_{RF} = 3 m and HE400M, except for the 3-story MRF (H_{RF} = 1 m, HE260M) and the 12-story MRF (HE600M).

^b Spacings and additional design variables were determined according to EN1992-1-1 and EN1994-1-2 design requirements.

^c Design approach: columns that attained their axial capacity are removed.

progressive collapse resistance.

The 9-story MRF was successfully retrofitted ($\lambda_{max}>1$) with the roof-truss and the column encasement. The roof-truss ensured a sufficient performance increase by redistributing loads to the perimeter columns. The 1st story columns of the existing MRF are critical at λ_{max} . Therefore, the encasement effectively enhanced the performance of the MRF, and collapse occurred at $\lambda_{max}>1$ owing to buckling of the internal columns at the 4th story. The bracing system was ineffective due to the buckling of the two columns adjacent to the removed column.

The 12-story MRF was successfully retrofitted ($\lambda_{max}>1$) with the roof-truss and the column encasement. The roof-truss redistributes loads to the perimeter columns, and the buckling of 1st story columns becomes critical only for $\lambda_{max}>1$. The encasement of the 1st story columns was locally effective, but the encasement of the 4th story columns was also necessary to obtain $\lambda_{max}>1$. Collapse occurred at $\lambda_{max}>1$ owing to buckling of the internal columns at the 2nd story. For the bracing system, the redistribution capacity was limited regardless of the design and did not reach $\lambda_{max}>1$.

The 15-story MRF was successfully retrofitted ($\lambda_{max}>1$) with the column encasement. The encasement effectively retrofitted the 1st story columns, and collapse occurred at $\lambda_{max}>1$ due to the buckling of the internal columns at the 4th story. The roof-truss and the bracing system were ineffective, regardless of the design, and buckling of the 1st story columns caused the collapse of the MRF.

It should be noted that, although considered ineffective, the assessments for the bracing system in the 9- and 15-story MRFs showed that, in some particular cases (i.e., $\phi_{\rm br}=100$ mm and $\phi_{\rm br}=180$ mm, respectively), the structures could retain some residual capacity and were able to redistribute the loads even after buckling of the columns. In fact, after buckling was observed in the columns adjacent to the removed member at λ < 1, loads were redistributed, and could be slightly increased to reach a higher load level for $\lambda_{max} > 1$. Fig. 11 shows the axial forces of the columns in the 9-storey retrofitted MRF with a bracing system with $\phi_{\rm br}$ = 100 mm. The Work Ratio (WR) (i.e., the demand-to-capacity ratio) of the 1st story columns is compared with the load factor evolution of the 9-story MRF. The WRs increase for the internal columns, i.e., Col 2 and Col 4, and reach their maximum for a displacement of approximately 0.01 m and λ < 1. Successively, due to buckling, such columns are unloaded, and the forces are transferred to the perimetral columns, i.e., Col 1 and Col 5. Simultaneously, a marked change in the stiffness of the λ - δ response is observed, and the load factor increases until a load factor $\lambda_{max} > 1$ is reached.

Based on the above discussion, it is evident that the bracing system may favor a ductile buckling mechanism over a brittle one, allowing further load increase after the internal columns buckle. This mechanism assumes that the columns that attain their buckling resistance continue

to act as supports, albeit with decreasing stiffness, to the bracing system. However, such a situation might not be acceptable in the design stage; therefore, it was assumed that the bracing system cannot be designed to retrofit the 9- and 15-story MRFs.

5.2. Redistribution capacity

Fig. 12 shows the distribution of the axial forces in the columns for the existing and retrofitted 9-story MRFs. The 9-story MRF was selected as the load distributions at the same state, *i.e.*, the application of the target loads at $\lambda=1$, could be compared, although such a load factor was achieved only after the buckling of internal columns in the MRF retrofitted with the bracing system. Only Column Lines 1, 2, and 3 (see Fig. 2) are shown, owing to symmetry conditions. Fig. 12 shows that the collapse of the existing structure, occurring at $\lambda=0.98$, is related to the attainment of the buckling resistance N_b in the 1st story column in Column Line 2. For simplicity, the buckling resistance according to EN-1993-1-1 [43] was considered for the columns at higher stories, *i.e.*, $N_b=N_{b,Rd}$.

The bracing system (red lines in Fig. 12) provides additional stiffness/strength to the 2nd story. Compared with the non-retrofitted configuration, loads in the central column line, *i.e.*, Column Line 3, increase in the columns above the stiff story. Columns above the 2nd story are less stressed in Column Line 2, while some loads are redistributed to the perimetral column in Column Line 1.

The roof-truss (blue lines in Fig. 12) introduces a stiffer zone on the top of the structure. Loads in the central column line hang to such a stiffer zone, and forces diminish in the columns above the 1st floor, with tension forces appearing in the columns above the 6th floor. Particular attention should be paid to columns and connections, which might become critical as they are not typically designed to withstand significant tension forces. In this case, the strength and stiffness of the roof-truss should be designed to redistribute more loads to the less stressed columns [26], but local strengthening measures may still be needed. Compared with the bracing system, a larger portion of the loads is distributed to Column Line 1 and the columns in Line 2 at the higher stories.

The column encasement solution (green lines in Fig. 12) does not significantly change the stiffness and the axial load redistribution compared to the existing structure. The axial force arising only in the steel section, *i.e.*, neglecting the load carried by the concrete part, is shown in the column line plots for the encased 1st story columns, to be consistent with the existing MRF and those retrofitted with the other solutions. Owing to the distribution of part of the axial forces to concrete, the compressive force developing in the steel core section in the 1st story column in Line 2 is much lower than the buckling resistance N_b .

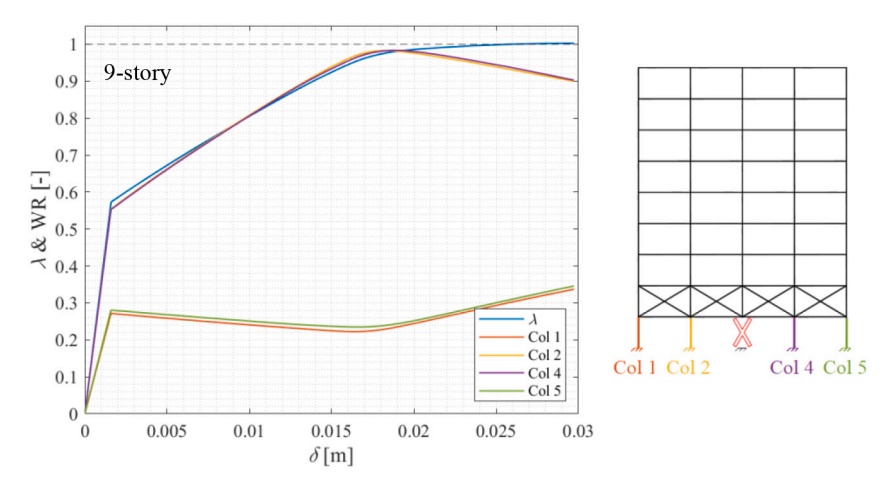


Fig. 11. WR of the 1st story columns of the 9-story MRF retrofitted with the BR.

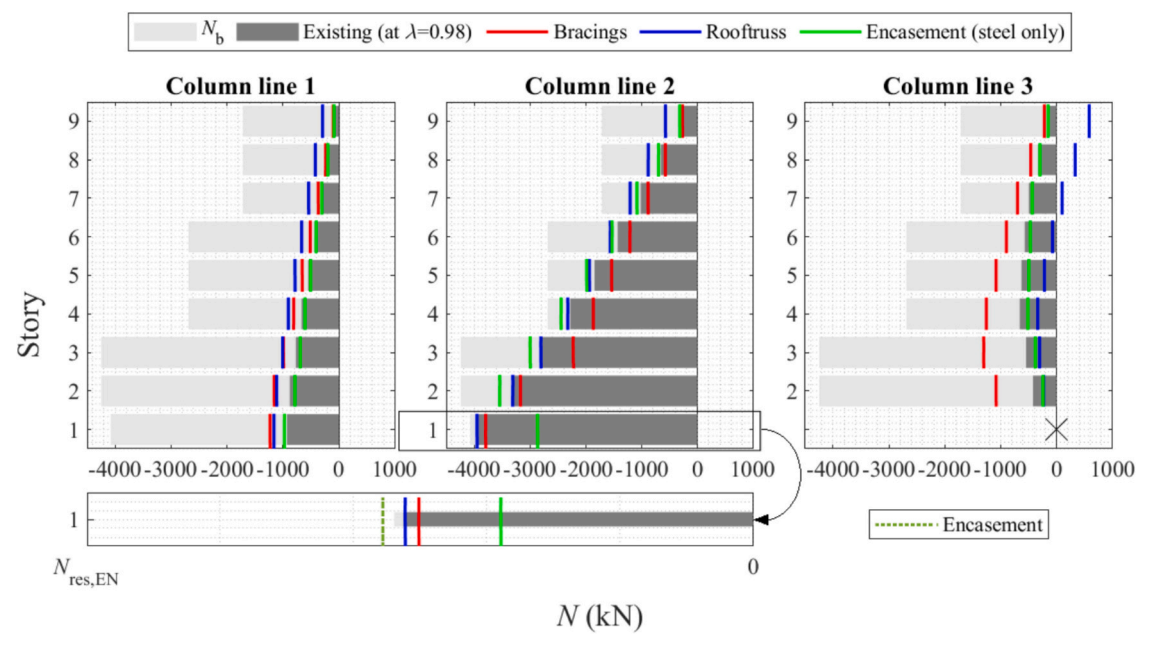


Fig. 12. Column loads distribution at collapse for the existing and at $\lambda = 1$ for the retrofitted 9-story MRFs.

For clarity, the overall actions on both concrete and steel (dashed lines in Fig. 12) are also shown for the critical column in the existing MRF, *i.e.*, the 1st story column in Line 2. The axial force is higher than that measured in the steel section only, but much lower than the resistance of the encased column $N_{\rm res,EN}$ at 28 days, according to Eurocode 4 [52]. The axial forces in the 1st story encased columns are 865 kN and 4208 kN for the 1st and 2nd column lines, respectively, which are 11 % and 56 % of $N_{\rm res,EN}$.

Fig. 13(a) provides an overview of the utilization of the 1st story columns of the retrofitted MRFs, by showing the WRs of the columns at λ

= 1. For the bracing system, WRs are significantly lower than for the other MRFs in the 3-story MRF, as this frame is not sensitive to column buckling. The 9- and 15-story MRFs exhibit higher WRs; however, in this case, the central columns have already experienced buckling at $\lambda < 1$, with part of their load being redistributed to the perimetral columns. For the roof-truss, the WRs for the 3-story MRF are similar to those provided by the bracing system. Conversely, for the other MRFs, the WRs are close to 1 in the central columns, as column buckling will cause the collapse for $\lambda > 1$. For the column encasement, the WRs are shown for the steel sections only. The WRs of the steel columns in the 9-, 12-, and 15-story

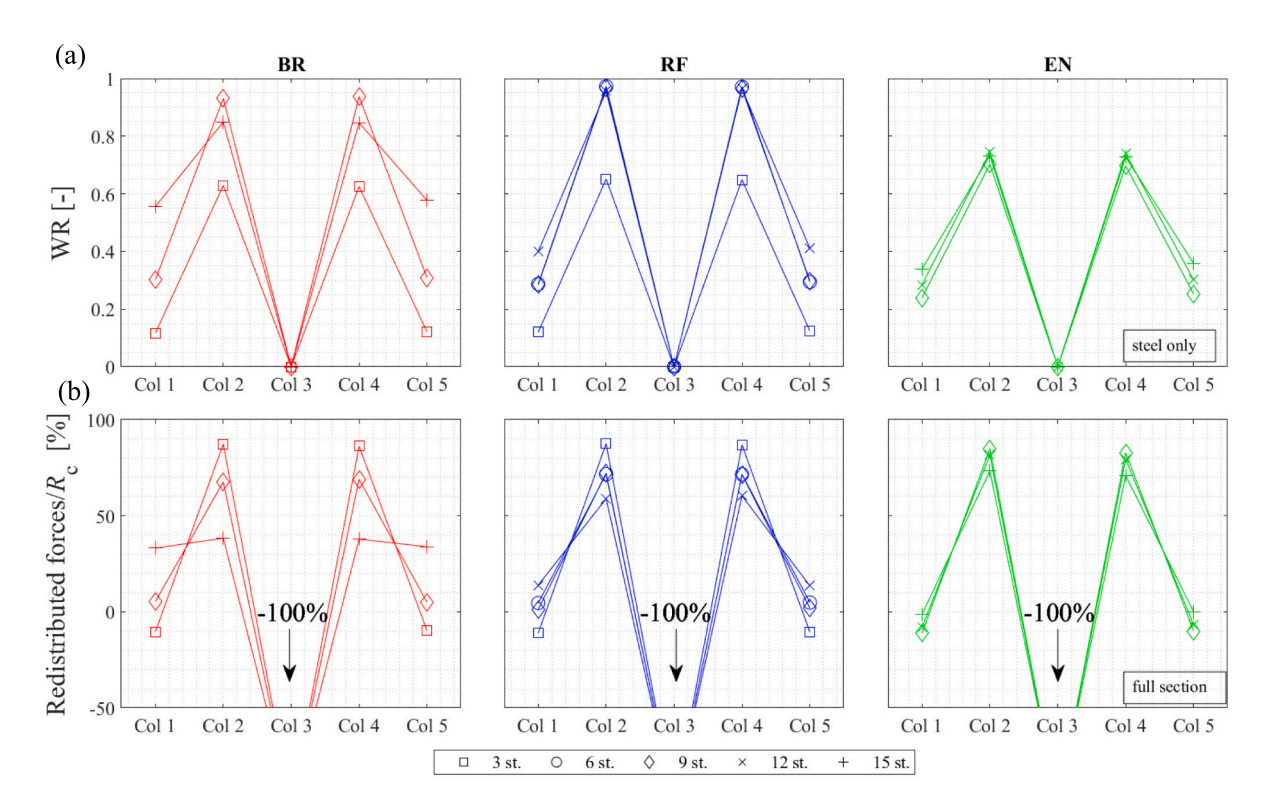


Fig. 13. (a) WRs and (b) redistribution of the vertical loads of the 1st story columns at $\lambda = 1$.

MRFs are significantly lower than 1, indicating that the column encasement effectively prevents column buckling in these MRFs.

Fig. 13(b) shows the loads redistributed during the removal phase in the 1st story columns of the retrofitted MRFs at a load factor $\lambda = 1$. The loads are normalized by the reaction forces R_c , previously carried by the central column, i.e., Col 3, immediately before its removal. Notably, for each retrofitted MRF, the sum of the redistributed values shown is greater than zero, reflecting the contribution of dynamic effects (captured by the Dynamic Increase Factor, DIF), which increases the total load demand on the remaining columns. The bracing system was designed to suppress the beam mechanism, thereby limiting the need for significant redistribution. Hence, vertical loads are primarily transferred to the two adjacent columns, i.e., Col 2 and 4, which also absorb part of the loads initially supported by the outer columns, i.e., Col 1 and 5. For the 9- and 15-story MRFs, the bracing system ensured a more even redistribution of the loads. However, such redistributions were achieved only after the buckling of the central columns; therefore, the prebuckling redistribution capacity of the bracing system should be considered limited compared to the roof-truss. The roof-truss for the 3story MRF was designed with the same purpose as the bracing system for the 3-story MRF, i.e., preventing the beam mechanism, and exhibits a similar redistribution capacity. For the other MRFs, the redistribution capacity is increased, especially for the 12-story MRF, where a stiffer roof-truss was designed to ensure more even redistribution. Finally, the column encasement consistently shows the lowest redistribution capacity among the retrofit measures, as it does not introduce additional paths to transfer loads from the removed to the other 1st story columns.

5.3. Influence of dynamic effects

Retrofit measures can modify critical structural parameters—such as stiffness and mass—that influence the dynamic response of the structure. While increasing capacity, retrofit measures may also impact demand, and hence careful considerations are required in this regard [26]. The influence of retrofitting on the dynamic response of the MRFs is evaluated with the numerical procedure suggested by Possidente et al. [42]. The procedure involves a comparative analysis of the response parameters between the non-linear static and dynamic analyses.

The non-linear static response is obtained through pushdown analyses, where the gravity loads are incrementally applied until collapse occurs

The non-linear dynamic analyses are performed in an Incremental Dynamic Analysis (IDA) fashion, increasing the load factor λ in each analysis until the target load factor $\lambda = 1$ is reached. The dynamic analyses are carried out using a procedure that resembles that described in Section 3.1, except that no DIF is considered, and the removal force F_c is applied dynamically. For this, the removal force F_c was linearly applied within the removal time defined as $t_{\rm rem} = (1/11T_{\rm v})$ following the recommendation of the GSA [12], where T_v represents the period corresponding to the 1st vertical vibration mode of the structure. For the dynamic analyses, the FE models were refined to incorporate 33 lumped masses distributed along the beams at each story level, as illustrated in Fig. 2(a). Additionally, Rayleigh damping with a damping ratio ξ equal to 5 % was implemented for the entire structure and defined for the two representative modes of vibrations for the analyzed problem, consisting of: 1) the first vibration mode; 2) the first vertical vibration mode, which involves the area above the removal [26,42]. Ten dynamic analyses with increments of the load factor λ of 0.1 were considered. The mass varied according to the load factor, and therefore, modal analyses were performed for each load factor to determine the vibration periods and, in turn, the removal time t_{rem} , and the coefficients for the Rayleigh damping.

Two response parameters relevant to beam and column mechanisms were selected: i) the axial force within the column adjacent to the removal N, and ii) the displacement above the removal δ .

For comparison purposes, the procedure was applied to the 9-story

MRF. Fig. 14 shows the time history of both response parameters from the dynamic analyses of the existing and retrofitted MRFs. The plots show the results of the *removal phase*, starting from the end of the *restoring phase*. The different curves refer to different load factors λ , and the dots represent the peak value reached in each analysis.

Fig. 14(a) shows that higher axial forces appear in the column for higher load factors λ , both at the beginning and during the *removal phase*. The load factor λ also affects the vibration period, as higher loads are associated with higher masses. As a consequence, the peak values occur for higher times when λ is increased. However, higher axial forces imply that buckling occurs earlier for higher load factors. Therefore, the peak value is reached at an earlier step when buckling is observed for $\lambda=0.9$ and $\lambda=1$ in the existing MRF and in the MRF retrofitted with the bracings and the roof-truss, respectively. As expected, the axial force in the column for the existing MRF, the MRF with a bracing system, and the case with the roof-truss is limited by the buckling resistance $N_{\rm b}$, representing the main limitation to reaching higher load factors. Conversely, the encasement provides the column with a higher buckling capacity, permitting higher axial forces and, hence, higher load factors.

Fig. 14(b) shows that higher load factors λ lead to larger vertical displacements δ , both at the beginning and during the *removal phase*. When λ is increased, higher vibration periods are observed, and the peak values occur for higher times, with no limitation on the measured displacement. However, for the existing MRF, the displacement diverges for $\lambda=1$, and a peak displacement cannot be identified. This indicates that the MRF eventually collapses, confirming the need for retrofitting. As expected, the bracing system and the roof-truss reduce the vertical displacement, and the MRFs retrofitted with these measures exhibit significantly smaller peak displacements compared to the existing structure. Conversely, the MRF retrofitted with concrete-encased columns exhibits displacement patterns similar to those of the existing MRF, but without leading to collapse.

Dynamic effects are evaluated for the peak dynamic response as the ratio between the load factor applied in the dynamic analysis $\lambda_{\rm D}$, and the load factor required to obtain the same response in the static analysis $\lambda_{\rm S}$. Hence, multiplying the loads by this ratio, the peak response of dynamic analyses can be obtained with simpler non-linear static analyses. With the same purpose, the UFC [11] provides dynamic increase factors, *i.e.*, DIFs, that apply only to the loads on the bays above the removed column. Hence, to enforce consistency, equations based on static schemes are employed to derive DIFs from the ratio between $\lambda_{\rm D}$ and $\lambda_{\rm S}$ [42]. For a central column loss, the following equations are used:

$$\begin{aligned} \operatorname{DIF}_{N}(\overline{N}) &= 57 \left/ 40 \bullet \frac{\lambda_{S}(\overline{N})}{\lambda_{D}(\overline{N})} - 17 \right/ 40; \\ \operatorname{DIF}_{\delta}(\overline{\delta}) &= 13 \left/ 16 \bullet \frac{\lambda_{S}(\overline{\delta})}{\lambda_{D}(\overline{\delta})} + 3 \right/ 16 \end{aligned} \tag{6}$$

where \overline{N} and $\overline{\delta}$ are the peak dynamic axial force and displacements at which the load factors are being compared. This procedure provides DIFs that are appropriate depending on the checked parameter, *i.e.*, N or δ , while a single value is recommended in the UFC [11].

Fig. 15 shows the DIFs derived for the existing and retrofitted frames. The evolution of the DIFs with the load factor exhibits an initial and approximately constant branch associated with an elastic response of the MRFs, followed by a sharp decrease as the MRFs exhibit non-linear behavior. In the elastic branch, the DIF values are influenced by the effects of geometrical non-linearities and the energy dissipated through various damping mechanisms [42,53]. The bracing system and the roof-truss allow additional energy dissipation, thereby enabling enhanced mitigation of the dynamic effects, *i.e.*, lower DIF values. Additionally, by redistributing the loads, these retrofit measures enable the MRF to remain in the elastic range for higher load factors. Hence, two beneficial effects are observed by implementing these measures: *i)* reduction of the dynamic effects when the structural response is essentially elastic, and

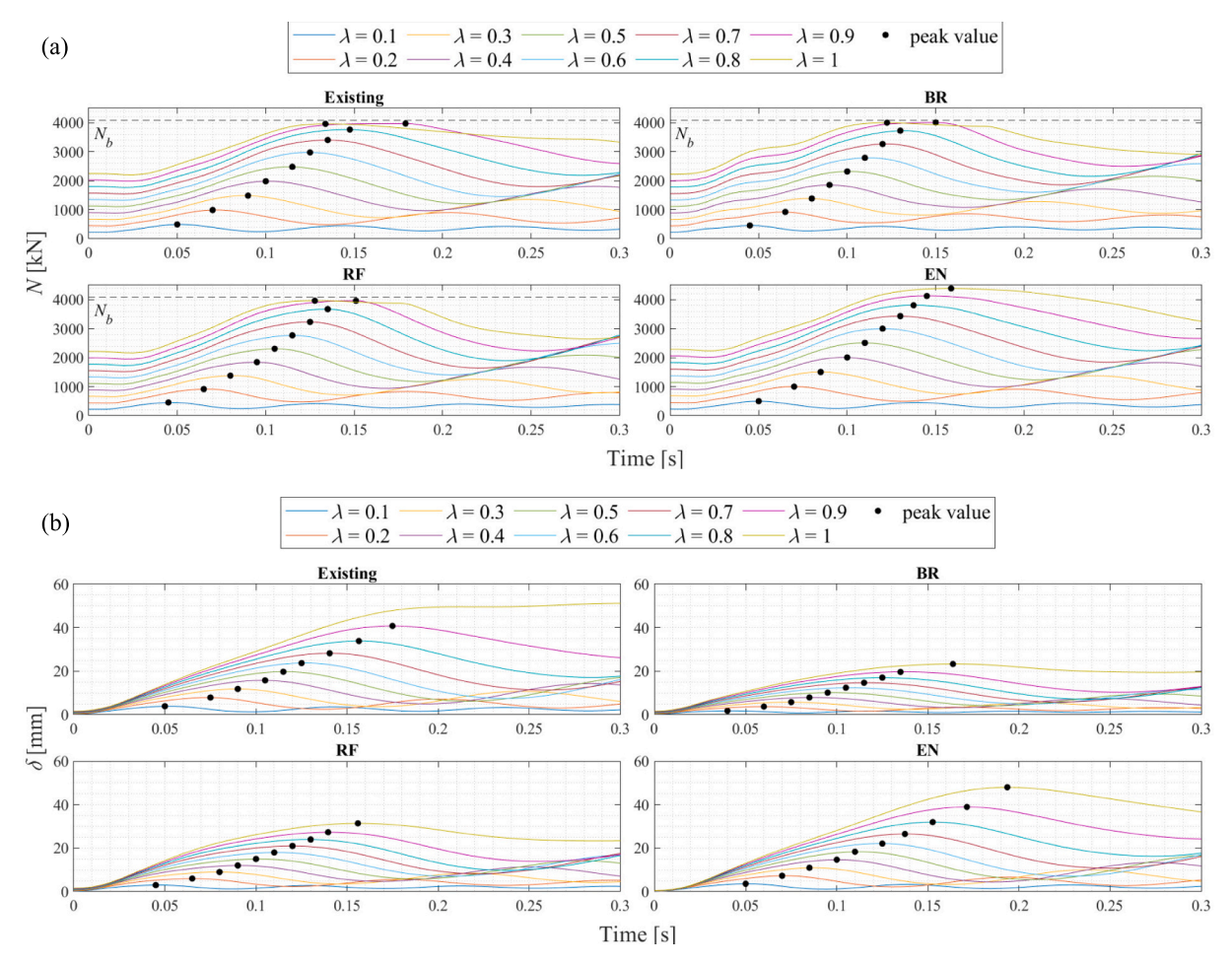


Fig. 14. IDA: (a) axial force in the columns adjacent to the removal; (b) displacement above the removal.

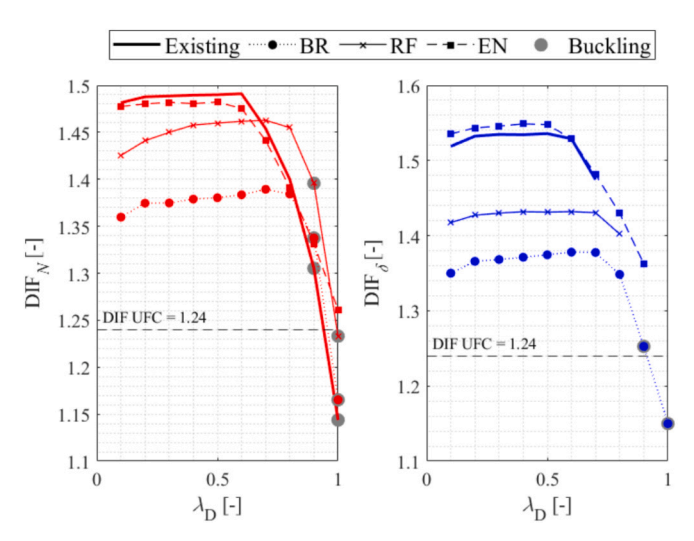


Fig. 15. Dynamic increase factors for the existing and retrofitted 9-story MRFs.

ii) the delay in the non-linear behavior that eventually leads to the collapse of the frames. The structure with encased columns exhibits DIFs that are very close to those of the existing frame. However, a less significant reduction of the DIF occurs for higher load factors as column buckling is prevented and the effects of geometrical non-linearities in the 1st story columns are diminished. In general, it can be concluded that while global measures may have a relevant impact, local measures

typically show a limited effect on the dynamic behavior of the building.

It is also useful to discuss the consequences of the observed response on the design process. In general, a MRF in need of retrofit exhibits a marked non-linear response before collapsing for load factors $\lambda < 1$. Fig. 15 shows that for load factors λ close to 1, the calculated DIF_N of the existing MRF for the critical parameter N is lower than the DIF_N evaluated according to the UFC [11]. Hence, the typical static procedure, relying on static analyses with loads increased by the DIF from the UFC, is conservative. However, due to the delay in the non-linear behavior (ii), the DIF_N observed for the bracing system and the roof-truss at the target design load factor, i.e., $\lambda = 1$, are higher than those of the existing MRF. The DIF_N is even higher than that of the UFC in the case of the column encasement. These results highlight that, while the design of the retrofit measures can be based on static analyses, dynamic analyses are still required to account for the dynamic effects that might increase the demand in the retrofitted structure.

5.4. Combination of measures

The effectiveness of strategies consisting of individual retrofit measures was assessed. However, it is worth noting that more extensive analyses involving, for instance, costs or sustainability aspects may reveal that the optimal solution consists of a combination of multiple measures. Furthermore, a combination of two measures that are individually ineffective may be preferred to a single effective measure. Detailed analyses encompassing costs and sustainability of the retrofit strategies are outside the scope of this work. However, as an illustrative example, some considerations regarding the material usage of the retrofit strategies are provided here for the 6-story MRF.

Fig. 16 shows the response of the retrofitted 6-story MRF, considering both isolated strategies and a combination of column encasement and bracing system. The figure also provides the weights of both the steel $W_{\text{ret,ST}}$ and the reinforced concrete $W_{\text{ret,RC}}$ used for the retrofitting. The existing 6-story MRF was subjected to a beam mechanism, but also showed significant stresses at the internal 1st story columns. For this structure, the target performance (i.e., $\lambda > 1$) could be achieved only with the roof-truss. Nevertheless, the combination of the bracing system and column encasement could represent a more effective and efficient solution to achieve progressive collapse capacity. The bracing system may be designed with a reduced bracing diameter, with the sole purpose of shifting the critical zone from the beam end to the columns, while relying on local strengthening to increase the capacity of the columns. Fig. 16 shows that the combination of these two measures is successful, whereas they are not effective when used separately. Compared with the roof-truss, a better performance and a lower overall weight increase are achieved.

5.5. Practical implementation

Fig. 17 provides an overview of the merits and limitations of individual retrofitting strategies. In addition to the effectiveness of various retrofit solutions in improving progressive collapse performance, redistributing vertical loads, and mitigating dynamic effects, further aspects regarding practical implementation are considered, providing a more holistic assessment of the solutions.

The retrofit measures showed their effectiveness depending on the collapse mechanisms. The bracing is suited to prevent beam mechanisms, which are typically observed in low-rise structures. The roof-truss system is effective against both beam and column mechanisms in low- to mid-rise buildings. The column encasement prevents only column mechanisms, which are more common in mid- to high-rise structures. However, besides the effectiveness of the retrofit measures depending on the characteristics of the buildings, their effectiveness may vary depending on the scenario, i.e., for different element loss scenarios. A column loss at the 1st story was considered, assuming a scenario that maximizes the risk; however, retrofit measures may need to be effective for other relevant scenarios, e.g., at higher stories. The bracing system is effective when placed on the story immediately above the column loss, and its effectiveness is limited if the column loss is located at lower stories. Conversely, the roof-truss represents a more versatile solution and may be effective against several column loss scenarios. The column encasement is a local measure and only enhances the capacity of the retrofitted columns; therefore, it has no effect if columns at different stories become critical.

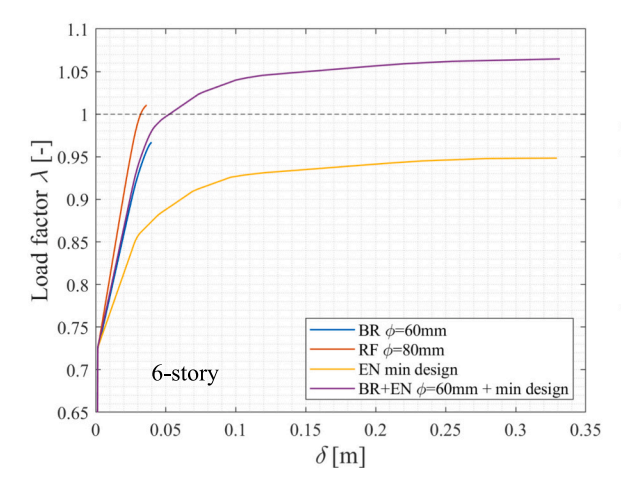
The design versatility of the retrofit measure may enable tailored solutions to meet the unique challenges posed by different structures. For the bracing system, this represents a key limitation as only the diameter $\phi_{\rm br}$ or the configurations of the braces can be modified, e.g., V or inverse V [23] or buckling restrained braces [25], with limited effect on the transfer mechanisms activated or, in general, the enhancement of progressive collapse capacity. Conversely, the roof-truss adds to the design options of the bracing system, and the dimensions of the members and the system height can be adjusted to increase the stiffness and strength of the retrofit measure, thereby improving its ability to redistribute loads to the farther columns [26]. The column encasement features a versatile design, allowing for various concrete and rebar dimensions to be considered, thereby increasing the columns' capacity. Nevertheless, once the column buckling is prevented, no additional benefits are introduced with design modifications.

Aspects such as costs, potential business interruption, and sustainability should be considered when selecting the optimal retrofit measure (Fig. 17). The bracing system has a lower cost compared to the rooftruss; however, for most cases, the cheapest solution is the concrete encasement. Additionally, measures implemented within the building, such as the column encasement and the bracing system, have a greater influence on the ordinary functions of a building. This may lead to practical problems in implementing the retrofit, including the relocation of occupants, prolonged business interruptions, and the related indirect costs. Conversely, the roof-truss has a very limited effect on ordinary functions as it is installed at the top and externally to the building. Finally, although more detailed sustainability considerations should be accounted for, it is worth noting that a sufficient capacity increase was achieved with lower material usage for the bracing system and column encasement. The roof-truss required a higher use of materials, implying a higher environmental impact.

In a more holistic perspective, embracing the detailed analysis of different hazards, additional aspects may influence the decision process for the best retrofit strategy. For instance, measures such as the column encasement might also help mitigate against impact or fire-induced progressive collapse by effectively protecting the steel columns [54]. Conversely, bracing systems may negatively affect the seismic behavior of MRFs by influencing their lateral response. These risk-related aspects warrant detailed future evaluation.

6. Conclusions

This study examines the design and performance of three retrofit strategies for existing multi-story steel-framed structures, aiming to mitigate the risk of progressive collapse. The investigation considered



	BR	RF	EN	BR+EN
Load factor (λ _{max})	0.97	1.01	0.95	1.06
W _{ret,ST} [ton]	1.43	21.89	0	1.43
W _{ret,RC} [ton]	0	0	7.14	7.14

Fig. 16. Performance and weights of the 6-story MRF with single and combined retrofit strategies.

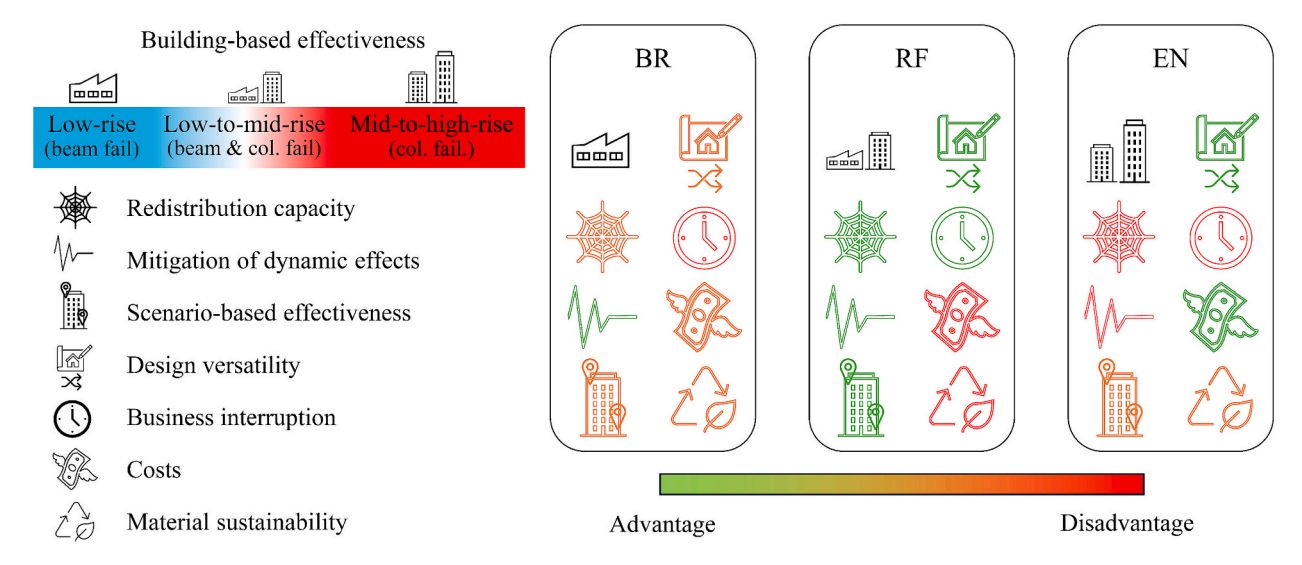


Fig. 17. Overall merits of the considered retrofit measures.

five steel Moment Resisting Frames (MRFs) ranging from low- to highrise structures, susceptible to either beam or column mechanisms under a column loss scenario. The retrofit strategies comprise global interventions, such as a horizontal bracing system installed above the removal zone and a rooftop-level truss system ('roof-truss'), as well as a local intervention involving the strengthening of first-story columns through concrete encasement. Static analyses were first conducted to assess the effectiveness of the different solutions and their ability to address the two collapse mechanisms. Dynamic analyses were successively carried out to evaluate the influence of retrofitting on the dynamic response and quantify the associated Dynamic Increase Factors (DIFs). The results indicate that retrofit effectiveness depends primarily on load redistribution capacity, building height, and the governing collapse mechanism (e.g., beam or column failure). Global strategies generally offer the most favorable impact on dynamic performance. However, no single solution proves universally effective, highlighting the need for case-specific approaches tailored to each structure's vulnerabilities. The study offers valuable insights and practical guidance to support more informed and comprehensive retrofit design decisions. The following main conclusions can be drawn:

- The bracing system effectively delays the onset of beam mechanisms but is generally insufficient for retrofitting structures where collapse is governed by column failure. The roof-truss system performs well against both beam and column mechanisms; however, it cannot prevent collapse due to buckling in first-story columns, especially in high-rise buildings with heavily stressed vertical elements. In contrast, concrete encasement of columns successfully mitigates buckling-related failures but does not address collapse mechanisms driven by beam failure.
- The bracing system offers fewer design options compared to other retrofit strategies. Design iterations highlighted the need for careful assessment of compressive forces in columns above the removal zone, which may exceed their buckling capacity. Being less materialintensive than the roof-truss solution, this strategy may be preferred for its lower economic and environmental impact.
- The roof-truss solution offers a versatile design, incorporating vertical, horizontal, and diagonal members that can be tailored to increase stiffness and improve load redistribution to distant columns. Design iterations highlighted the importance of carefully assessing tension forces in columns and connections above the removal zone. This strategy effectively mitigates progressive collapse across

- different story levels and, being externally installed, has minimal impact on the building's regular functions.
- The design of concrete encasements varies depending on the configuration of steel and concrete components, yet even the minimum design consistently provides effective local column strengthening. As a local intervention, encasement does not facilitate load redistribution or mitigate dynamic effects. However, this solution remains economically attractive due to lower material costs.
- While each retrofit strategy has distinct advantages, combining global and local measures can yield optimal performance and material efficiency. Global interventions can be tailored to address specific collapse mechanisms, while local strengthening targets critical vulnerabilities. For instance, in the 6-story MRF, a combined bracing—column encasement approach outperformed the roof-truss solution, achieving better structural performance with significantly lower added weight. In contrast, bracing or encasement alone did not provide sufficient enhancement.

The present study investigated the effectiveness of retrofit strategies for structures governed by different mechanisms and provided a critical overview of their benefits and drawbacks. Despite higher costs and environmental impact, the roof-truss emerged as the overall most effective and versatile measure, with limited influence on ordinary functions. 2D frames were considered to focus on the contributions provided and the mechanisms activated with the retrofit measures. Future studies will consider the beneficial contribution to robustness provided by transverse steel frames or concrete slabs, while devising effective global spatial measures within an overall integrated risk framework that accounts for economic and environmental considerations. To further generalize the outcomes, structures with different characteristics and designed according to other design codes will be considered.

CRediT authorship contribution statement

Luca Possidente: Writing – original draft, Visualization, Validation, Methodology, Investigation, Formal analysis, Conceptualization. Fabio Freddi: Writing – review & editing, Supervision, Project administration, Methodology, Funding acquisition, Conceptualization. Ahmed Y. Elghazouli: Writing – review & editing, Supervision, Methodology, Conceptualization.

Declaration of competing interest

The authors declare the following financial interests/personal relationships which may be considered as potential competing interests:

Luca Possidente and Fabio Freddi report financial support was provided by UK Research and Innovation. If there are other authors, they declare that they have no known competing financial interests or personal relationships that could have appeared to influence the work reported in this paper.

Acknowledgements

This research is supported by the UK Research and Innovation Institution (UKRI) in the framework of the project RESTORE "Retrofit strategies for Existing STructures against prOgRessive collapse" (grant EP/X032469/1). Any opinions, findings, and conclusions or recommendations expressed in this paper are those of the authors and do not necessarily reflect the views of UKRI.

Data availability

Some or all data, models, or code that support the findings of this study are available from the corresponding author upon reasonable request.

References

- J.M. Adam, F. Parisi, J. Sagaseta, X. Lu, Research and practice on progressive collapse and robustness of building structures in the 21st century, Eng. Struct. 173 (2018) 122–149
- [2] C. Pearson, N. Delatte, Ronan point apartment tower collapse and its effect on building codes, J. Perform. Constr. Facil. 19 (2) (2005) 172–177.
- [3] M.A. Sozen, C.H. Thornton, W.G. Corley, P.F. Mlakar, The Oklahoma city bombing: structure and mechanisms of the Murrah building, J. Perform. Constr. Facil. 12 (3) (1998) 120–136.
- [4] Z.P. Bazant, M. Verdure, Mechanics of progressive collapse: learning from world trade center and building demolitions, J. Eng. Mech. 133 (3) (2007) 308–319.
- [5] C. Pellecchia, A. Cardoni, G.P. Cimellaro, F. Ansari, A.A. Khalil, Progressive collapse analysis of the Champlain towers south in surfside, Florida, J. Struct. Engineer. (United States) 150 (1) (2023) 04023211.
- [6] FEMA 426, Reference Manual to Mitigate Potential Terrorist Attacks against Buildings, 2003 (December).
- [7] S. El-Tawil, H. Li, S. Kunnath, Computational simulation of gravity-induced progressive collapse of steel-frame buildings: current trends and future research needs, J. Struct. Engineer. (United States) 140(8): A2513001 (2014) 1–12.
- [8] C. Dimopoulos, F. Freddi, T.L. Karavasilis, G. Vasdravellis, Progressive collapse of self-centering moment resisting frames, Eng. Struct. 208 (2020) 109923, https:// doi.org/10.1016/j.engstruct.2019.109923.
- [9] M. Kierat, F. Freddi, Numerical study on the progressive collapse of cable-stayed columns due to cable loss, Thin-Walled Struct. 215 (Part A) (2025) 113439, https://doi.org/10.1016/j.tws.2025.113439.
- [10] European Committee for Standardization (CEN) Eurocode 1, Actions on structures – Part 1–7: General actions – Accidental actions, in: European Standard EN 1991–1–7, Brussels, Belgium, 2006.
- [11] DOD (United States Department of Defense), Unified Facilities Criteria (UFC) Design of Structures to Resist Progressive Collapse. 4–023-0314. July 2009 – Change 3, 1 November 2016, Arlington, Virginia, 2016.
- [12] GSA, Progressive Collapse Analysis and Design Guidelines for New Federal Office Buildings and Major Modernisation Projects, General Services Administration, Washington, DC, 2003.
- [13] European Commission, A Renovation Wave for Europe Greening our Buildings, Creating Jobs, Improving Lives. Brussels, Belgium, 2020.
- [14] F. Kiakojouri, V. De Biagi, B. Chiaia, M.R. Sheidaii, Strengthening and retrofitting techniques to mitigate progressive collapse: A critical review and future research agenda, Eng. Struct. 262 (2022) 114274.
- [15] D. de Silva, A. Bilotta, E. Nigro, Experimental investigation on steel elements protected with intumescent coating, Constr. Build. Mater. 205 (2019) 232–244.
- [16] Z. Lu, K. Rong, Z. Zhou, J. Du, Experimental study on performance of frame structure strengthened with foamed aluminum under debris flow impact, J. Perform. Constr. Facil. 34 (2) (2020) 04020011.
- [17] A. Astaneh-Asl, E.A. Madsen, C. Noble, R. Jung, Use of Catenary Cables to Prevent Progressive Collapse of Buildings, Report number: UCB/CEE-STEEL-2001/02., Univ of California at, Berkeley, US, 2001.
- [18] Y.F. Zhu, C.H. Chen, L.M. Keer, Y. Huang, Y. Yao, Structural response and resilience of posttensioned steel frames under column loss, J. Constr. Steel Res. 158 (2019) 107–119.

- [19] G. Papavasileiou, N. Pnevmatikos, Optimised retrofit of steel-concrete composite buildings against progressive collapse using steel cables. 16th European Conference on Earthquake Engineering, 2018.
- [20] J. Chen, W. Peng, R. Ma, M. He, Strengthening of horizontal bracing on progressive collapse resistance of multistory steel moment frame, J. Perform. Constr. Facil. 26 (5) (2012) 720–724.
- [21] A. Naji, M.R. Ommetalab, Horizontal bracing to enhance progressive collapse resistance of steel moment frames, Struct. Des. Tall Special Build. 28 (5) (2019).
- [22] J. Jiang, G.-q. Li, Mitigation of fire-induced progressive collapse of steel framed structures using bracing systems, Adv. Steel Constr. 15 (2) (2019) 192–202.
- [23] F.H. Rezvani, M.A.M. Taghizadeh, H.R. Ronagh, Effect of inverted-V bracing on retrofitting against progressive collapse of steel moment resisting frames, Int. J. Steel Struct. 17 (3) (2017) 1103–1113.
- [24] M. Bandyopadhyay, A.K. Banik, Improvement of progressive collapse resistance potential of semi-rigid jointed steel frames through bracings, Int. J. Protect. Struct. 7 (4) (2016) 518–546.
- [25] H. Eletrabi, J.D. Marshall, Catenary action in steel-framed buildings with buckling restrained braces, J. Constr. Steel Res. 113 (2015) 221–233.
- [26] F. Freddi, L. Ciman, N. Tondini, Retrofit of existing steel structures against progressive collapse through roof-truss, J. Constr. Steel Res. 188 (2022) 107037.
- [27] M. Ferraioli, B. Laurenza, A. Lavino, G. De Matteis, Progressive collapse analysis and retrofit of a steel-RC building considering catenary effect, J. Constr. Steel Res. 213 (2024) 108364.
- [28] S.J. Mirvalad, Robustness and Retrofit Strategies for Seismically-Designed Multistory Steel Frame Buildings Prone to Progressive Collapse, PhD Thesis,, Concordia University, Montreal, Canada, 2013.
- [29] K. Galal, T. El-Sawy, Effect of retrofit strategies on mitigating progressive collapse of steel frame structures, J. Constr. Steel Res. 66 (4) (2010) 520–531.
- [30] J.L. Liu, Preventing progressive collapse through strengthening beam-to-column connection, part 1: theoretical analysis, J. Constr. Steel Res. 66 (2) (2010) 229–237.
- [31] B. Ghorbanzadeh, G. Bregoli, G. Vasdravellis, T.L. Karavasilis, Pilot experimental and numerical studies on a novel retrofit scheme for steel joints against progressive collapse, Eng. Struct. 200 (2019) 109667.
- [32] S. Gerasimidis, C. Baniotopoulos, Progressive collapse mitigation of 2D steel moment frames: assessing the effect of different strengthening schemes, Stahlbau 84 (5) (2015) 324–331.
- [33] S. Mazzoni, F. McKenna, M.H. Scott, G.L. Fenves, Open System for Earthquake Engineering Simulation User Command-Language Manual, OpenSees Version 2.0, University of California, Berkeley, CA, 2009.
- [34] R. Zandonini, N. Baldassino, F. Freddi, Robustness of steel-concrete flooring systems. An experimental assessment, Stahlbau 83 (9) (2014) 608–613.
- [35] R. Zandonini, N. Baldassino, F. Freddi, G. Roverso, Steel-concrete composite frames under the column loss scenario: an experimental study, J. Constr. Steel Res. 162 (2019) 105527.
- [36] G. Roverso, N. Baldassino, R. Zandonini, F. Freddi, Experimental assessment of an asymmetric steel-concrete frame under a column loss scenario, Eng. Struct. 293 (2023) 116610.
- [37] B.A. Izzuddin, A.G. Vlassis, A.Y. Elghazouli, D.A. Nethercot, Progressive collapse of multi-story buildings due to sudden column loss — part I: simplified assessment framework, Eng. Struct. 30 (2007).
- [38] A.G. Vlassis, B.A. Izzuddin, A.Y. Elghazouli, D.A. Nethercot, Progressive collapse of multi-story buildings due to sudden column loss — part II: application, Eng. Struct. 30 (2007) 1424–1438.
- [39] F. Sadek, S. El-Tawil, H. Lew, Robustness of composite floor systems with shear connections: modeling, simulation, and evaluation, J. Struct. Eng. 134 (2008) 1717–1725.
- [40] S. Gerasimidis, C. Bisbos, C. Baniotopoulos, Vertical geometric irregularity assessment of steel frames on robustness and disproportionate collapse, J. Constr. Steel Res. 74 (2012) 76–89.
- [41] S. Gerasimidis, Analytical assessment of steel frames progressive collapse vulnerability to corner column loss, J. Constr. Steel Res. 95 (2014) 1–9.
- [42] L. Possidente, F. Freddi, N. Tondini, Dynamic increase factors for progressive collapse analysis of steel structures considering column buckling, Eng. Fail. Anal. 160 (2023) 108209.
- [43] CEN (European Committee for Standardization), Eurocode 3: Design of Steel Structures – Part 1–1: General Rules and Rules for Building, EN 1993–1–1. Brussels, Belgium, 2005.
- [44] CEN (European Committee for Standardization), Eurocode 8: Design of Structures for Earthquake Resistance. Part 1: General Rules, Seismic Action and Rules for Buildings, EN 1998–1. Brussels, Belgium, 2005.
- [45] CEN (European Committee for Standardization), Eurocode 1: Actions on structures – Part 1–1: General actions - densities, self-weight, imposed loads for buildings, EN 1991–1–1. Brussels, Belgium, 2002.
- [46] C.-H. Lee, S. Kim, K. Lee, Parallel axial-flexural hinge model for non linear dynamic progressive collapse analysis of welded steel moment frames, J. Struct. Eng. 136 (2) (2009) 165–173.
- [47] F. Dinu, I. Marginean, D. Dubina, I. Petran, Experimental testing and numerical analysis of 3D steel frame system under column loss, Eng. Struct. 113 (2016) 59-70
- [48] J.M. Castro, A.Y. Elghazouli, B.A. Izzuddin, Modelling of the panel zone in steel and composite moment frames, Eng. Struct. 27 (2005) 129–144.
- [49] F.A. Charney, W.M. Downs, Modeling procedures for panel zone deformations in moment resisting frames, in: Proc. Conference on Connections in Steel Structures V: Innovative Steel Connections, Amsterdam, the Netherlands, 2004.

- [50] L. da Rosa Ribeiro, F.C. Macedo, A.T. Beck, F. Parisi, Optimal risk-based design of planar RC frames under progressive collapse: influence of frame aspect ratio and column cross-section, Eng. Struct. 342 (2025) 120905.
- [51] CEN (European Committee for Standardization), Eurocode 2: Design of Concrete Structures – Part 1–1: General Rules and Rules for Building, EN 1992–1–1. Brussels, Belgium, 2003.
- [52] CEN (European Committee for Standardization), Eurocode 4: Design of Composite Steel and Concrete Structures. – Part 1–1: General Rules and Rules for Building, EN 1992–1–1. Brussels, Belgium, 2004.
- [53] M. Liu, A new dynamic increase factor for nonlinear static alternate path analysis of building frames against progressive collapse, Eng. Struct. 48 (2013) 666–673.
- [54] L. Possidente, F. Freddi, N. Tondini, Fire response of steel frames retrofitted against progressive collapse, Fire Saf. J. 153 (2025) 104371.